REPORT NO. M10550

Cooling System for Retrofitted Electric Mining Truck (EPCA-E100 project)

Results of research carried out as MRIWA Project M10550

at Electric Power Conversions Australia (EPCA)

by

Clayton Franklin

Date published May, 2026

Distributed by: MRIWA
1 Adelaide Terrace
Perth WA 6000
to which all enquiries should be addressed

Acknowledgements

This research was supported by the Minerals Research Institute of Western Australia (MRIWA) under its *METS Innovation Program* as Project M10550. The authors acknowledge the contributions of industry partners and researchers who provided technical expertise and support throughout the project.

MINISTER FOR MINES AND PETROLEUM
Hon David Michael MLA

CHIEF EXECUTIVE OFFICER, MINERALS RESEARCH INSTITUTE OF WESTERN AUSTRALIA
Nicole Roocke

LEAD INVESTIGATOR,
Clayton Franklin

AUTHORS:
Clayton Franklin
Muhummad Fazidan

REFERENCE
The recommended reference for this publication was:
APA7 format

REPORT DOI: 10.71342/359794298652

This report was available from the
National Library of Australia
ISBN: 978-1-925971-50-0
ISSN: 2203-2745

PARTICIPATING ORGANISATIONS

ABOUT THIS PUBLICATION
This report summarises work undertaken by Electric Power Conversions Australia (EPCA) to design, build and test a cooling system for a retrofitted battery-electric mining truck as part of MRIWA Project M10550.

KEYWORDS AND TAGS
electric haul truck, mining electrification, thermal management, cooling system, battery-electric retrofit

Published 2026 by the Minerals Research Institute of Western Australia
This report was published in digital format (PDF) and was available online at
https://www.mriwa.wa.gov.au/research-projects/project-portfolio/

CONTACT
Minerals Research Institute of Western Australia
1 Adelaide Terrace
Perth WA 6000
+61 8 6180 4340
mail@mriwa.wa.gov.au
https://www.mriwa.wa.gov.au/

Executive Summary

The global transition toward vehicle electrification has accelerated in recent years, driven by the need to reduce greenhouse gas emissions and adopt cleaner and more efficient energy sources. The global mining industry contributes to a large amount of diesel fuel consumption and has expressed interest in reducing its carbon emissions to meet the 2030 and 2050 net-zero targets set by the United Nations in the 2016 Paris Agreement.

Electric Power Conversions Australia (EPCA) has developed an innovative retrofitting approach that replaces diesel engines in heavy off-highway trucks, particularly the 100 tonne Caterpillar 777 model, with a full-battery electric powertrain to address the electrification transition needs. The retrofitting approach utilises a circular economy solution that presents various benefits, such as lower lifecycle emissions and lower capital and operational costs, with an enhanced vehicle performance as compared to its Internal Combustion Engine (ICE) counterpart.

This report presents the key technical challenges associated with implementing a fully electric-powered truck, focusing on its cooling system's design, development, and optimisation. An effective thermal management system was critical to maintaining the efficiency, longevity, and performance of the overall power electronic systems, such as the battery, electric motors, and other auxiliary components in the vehicle. The project scope was divided into four primary phases: preliminary design and thermodynamic modelling, manufacturing and installation, control system development and coding, and cooling system commissioning and testing.

The design of the cooling system accounts for the thermal performance needs of the newly added electric power train and the existing auxiliary components. The design aims to ensure the system operates within its safe and optimal temperature range, which was typically below high ambient. The next stage focuses on integrating the physical packaging of the cooling system into the Caterpillar 777D truck. Once the system was physically installed, the next step was to implement a control philosophy with software development. The software integrates the chiller with the VCU (Vehicle Control Unit) and the Human Machine Interface (HMU). Lastly, the system was load-tested at a mine site for data logging and design validation.

Through a systematic engineering approach, this project aims to develop and validate a robust thermal management system that ensures optimal thermal performance, proving the long-term viability and reliability of electric haul trucks in mining operations in the harsh climate conditions of mining sites in Australia. The findings and recommendations outlined in this report will contribute to the broader industry shift towards sustainable and high-performance electrification solutions in Australia.

Table of Contents

Terms, Abbreviations and Acronyms

Terms, Abbreviations, & Acronyms	Description
BTMS	*Battery Thermal Management System*
EPCA	*Electric Power Conversions Australia*
HMI	*Human Machine Interface*
HV	*High Voltage*
ICE	*Internal Combustion Engine*
LV	*Low Voltage*
OEM	*Original Equipment Manufacturer*
P&ID	*Piping & Instrumentation Diagram*
VCU	*Vehicle Control Unit*

List of Tables/Figures

1. Introduction

This last decade has shown a significant increase in the shift towards the electrification of vehicles in various industries globally. The transition was highly influenced by the need to reduce global greenhouse gas emissions and the move towards cleaner and more efficient energy use, particularly in vehicle transportation. In the last few years, the global mining industries have expressed interest in utilising electric-powered vehicles in their fleets to replace their existing combustion engine vehicles, motivated by the 2030 and 2050 net zero goals agreed upon by the United Nations in the 2016 Paris Agreement. In the mining industry, most energy consumed arises from diesel combustion, primarily heavy vehicles and machinery. Hence, the OEMs are incentivised to design and manufacture a cleaner alternative to their traditional combustion engine counterpart, such as a battery-powered vehicle, hydrogen fuel vehicle, trolley assist vehicle, and more.

EPCA prides itself on its circular economy approach of retrofitting existing diesel-powered engine trucks with full-battery electric-powered trucks. Such an approach not only reduces the carbon emissions in the overall life cycle of the truck but also provides a cheaper option in capital and operational investments with superior performance capability.

The following sections detail the electric-powered trucks' challenges, particularly with the cooling system design. With that, the appropriate solutions are derived and implemented throughout the project's duration, outlined in the following sections.

1.1. Minerals research/industry challenge and background

Building and operating a fully electric 100t haul truck presents a unique challenge that requires comprehensive, detailed design efforts and testing to ensure the truck was capable of operating in the harsh conditions of the mine sites in Australia. According to the Australian Bureau of Meteorology, the recorded temperature in the Pilbara region in Western Australia has reached up to 50.5°C . This presents a unique design challenge as some can only safely operate below this ambient temperature. In contrast to an internal combustion engine, a fully electric power vehicle has a lower allowable operating temperature for the power electronics and oftentimes will require an operating temperature below the ambient temperature. For example, the battery pack has an ideal operating temperature range between 20°C and 35°C to achieve the optimal power output while maintaining the maximum life of the battery pack. Therefore, an existing radiator cooling system in the original ICE vehicle was not a viable option to thermally manage the battery's operating temperature. Hence, the system will require a chiller unit to provide cooling below ambient, especially during hot summer, which can reach up to 50°C.

Moreover, a chiller unit will also have a higher ambient temperature limit before it starts to derate, reducing its cooling capacity. For example, a chiller unit may have a cooling capacity of 12kW at 40°C and have 10kW of cooling capacity at 50°C. Therefore, the chiller unit must be selected to be capable of providing the minimum required cooling capacity under the various conditions of a mine site.

1.2. Objectives of the research

This research aims to design and build a thermal management system for a 100t retrofitted battery electric haul truck. Before commencing any design and manufacturing work, it was essential to understand the thermal behaviour and requirements of the newly added power electronics system, such as the HV battery packs, drive motor and inverter, and the DCDC converter. The thermal management system must be designed to withstand and operate continuously in the hottest conditions seen in Australia. In the Pilbara region, the average monthly temperature frequently exceeds 40ºC, with the hottest day recorded at 50.7ºC. The system will be designed to operate effectively for an ambient temperature of 45ºC, with consideration given at ambient temperatures of up to 50ºC. The engineers shall review the thermal requirements and analytically develop a preliminary cooling circuit design and a numerical simulation model to predict the behaviour of these components and the truck's overall performance. The calculated and simulation results will inform the engineer regarding the performance viability of the vehicle and see if it can meet the minimum viable product requirements for the clients.

After the design stage, the engineers will build and assemble the prototype cooling system design for the truck. The system must be tested and verified against the predicted and calculated results in the design stage. The areas of improvement in the cooling system design are to be identified and will serve as a benchmark for future design work.

1.3. Scope

This project focuses on the design, installation, control system development, and validation of a cooling system for a retrofitted CTA 777D fully electric truck. The aim was to develop a robust and efficient thermal management system capable of effectively regulating the thermal conditions of high-load components such as drive motors, inverters, batteries, auxiliary drivelines, and transmission and brake heat exchangers. The project will ensure that the retrofitted electric truck operates reliably in harsh and demanding mining environments, minimising thermal stress and maintaining performance consistency over an extended period.

The objective of this project was to design and manufacture a cooling circuit that meets specific thermal management criteria based on the truck's operational demands. Moreover, a digital twin model was developed to understand the vehicle's overall performance based on the cooling system's performance. Once the design was completed and numerically validated, the system was manufactured, installed, and integrated into the retrofitted vehicle. Next, a control system will be programmed and developed to integrate the cooling systems with the truck's programmable logic controller system (PLC) and vehicle control unit (VCU). Lastly, rigorous tests are done at mining conditions to validate the cooling system's performance.

The effectiveness of the cooling system determines the project's success criteria. The cooling system should maintain the critical component temperatures within the safe operating ranges under all tested conditions. The system must be able to achieve flow distribution and pressure drop characteristics that meet the design parameters that are validated through field testing. A seamless integration with the VCU and PLC was crucial for the truck's operation. In conclusion, this project will ensure that the retrofitted electric mining truck maintains consistent performance while operating under extreme mining conditions, supporting the broader goal of sustainable and reliable mining operations through electrification.

2. Methodology

2.1. Preliminary Design and Thermodynamic Calculations and Modelling

The initial stage of the project was to complete the preliminary design and thermodynamic modelling of the cooling system. To start, the team must determine the critical components within the vehicle that require a thermal management system to maintain its optimal operating temperature. The components and their operating range are summarized in Table 1:

Table 1: Thermal System Design Constraints

Components	Operating Temperature Requirements	Cooling Requirements
1 Battery Pack	Discharge Temperature Range: -20°C to 60°C Charging Temperature Range: 0°C to 45°C Optimal Temperature for infinite Life: 20°C-35°C	Max Pressure of 1 bar Min Heat Rejection at 1C of Charging = 8728W Min Flow Rate at 1C of Charging = 83LPM
2 of Main Drive Motor	Maximum Water Temperature: 80°C Peak Performance Temperature: <45°C Mild Derate Temperature: 60°C to 80°C Zero Torque Temperature: 100°C	Flow Rate Range = 15 to 45LPM
2 of Main Motor Inverter	First Derating Temperature Range: 40°C to 80°C Derate to Zero Torque Temperature Range: 80°C to 100°C	Max Pressure of 3 bar Min Flow Rate of 24LPM
1 of Auxiliary Motor	Operating Temperature Range: -40°C to 120°C	Max 5 Bar

1 of Auxiliary Inverter	Max Inlet Coolant Temperature: 60°C	Minimum flow rate of 20LPM at 2 Bar
DCDC Converter	Operating Temperature Range: -40°C to 65°C Derating Temperature: 65°C to 85°C	Max Pressure of 2.5 Bar Nominal Flow Rate: 6LPM
Brake Oil Cooler	Operating Range Limit: 32°C to 124°C	N/A
Transmission Oil Cooler	Operating Range Limit: 45°C to 129°C	N/A

As detailed in Table 1, the tractive batteries have the lowest optimal operating temperature range of 20°C to 35°C, below the intended ambient temperature of the environment where the truck will operate. Therefore, active cooling through a BTMS unit was required to manage the battery pack's temperature below ambient. After the batteries, the two of the main motor inverters have the lowest first derating temperature of optimal operating temperature, where the inverter will start to derate by limiting the maximum current output when it hits 45°C until 80°C and will derate at a higher rate until it reaches 100°C where it reaches zero torque output. (See Fig. 1).

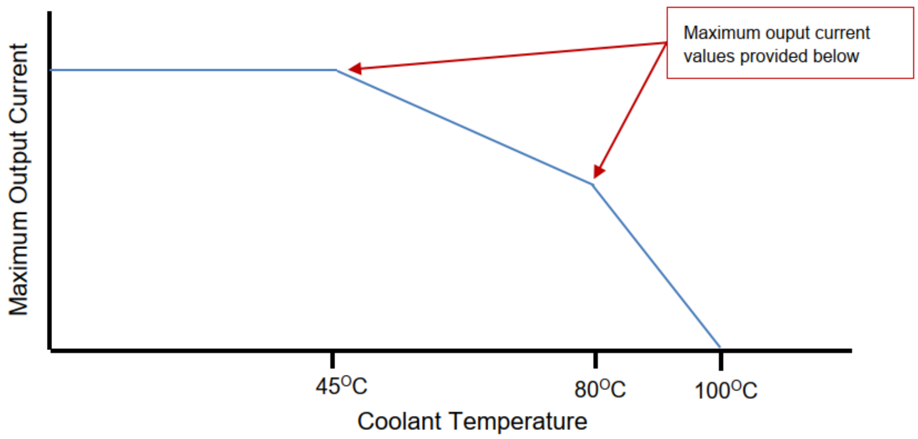

Figure 1: Drive Inverter Output Current vs Coolant Temperature

Table 2 showed the batteries' thermal properties under different C-rates provided by the battery manufacturer.

Table 2: Heat Generation Properties

C- Rate	Pack Current (A)	Heat Generated (W)	Minimum Heat Rejection (W)	Minimum Coolant Flow Rate (LPM)
0.25	111	849	39	2
0.5	223	3398	966	18
0.75	334	7645	3998	48
1.0	445	13591	8728	83
1.5	668	30580	23286	165

2.0	890	54364	44639	261

The cooling circuit was designed per the cooling requirements and coolant flow listed in Table 1 above. The cooling circuit was designed to be able to satisfy the specified requirements and additional criteria as listed below:

- A Fail-Safe approach was applied to the cooling circuit to ensure modular operability and functional reliability.
- Allow modular controllability of coolant delivery to all the components in the cooling system.

A 10 kW BTMS unit was implemented as the chiller for the cooling system. The chiller has 10kW of cooling capability and can operate at ambient temperatures between -35°C to 50°C. The six battery packs will generate the most significant amount of heat during charging at a 1C rate and will require a minimum heat rejection of 8.728 kW for each battery pack. During operation, it was estimated that the main motor and its inverter will deliver the highest heat generation of 32 kW. Hence, the cooling system must be able to reject at least 8.728 kW of heat generated during charging and 32 kW of heat generated from the motor during driving at peak load. Since the current vehicle only has one battery, the research team are limited by the power output into the drive motors. The lower battery power output translates to a lower heat generated during driving; Hence, the research team can get away with a smaller chiller unit for testing. The design considers the possibility of additional chillers integrated into the common manifold once more batteries are added to the vehicle.

The Piping and Instrumentation Diagram (P&ID) for one chiller system was detailed in Fig. 2 below. Refer to Appendix 1 for a larger view of the cooling circuit. The prototype cooling circuit was designed in a configuration that allows for one chiller to provide cooling to multiple components in a single circuit through common header manifolds. The pressure manifold will split the circuit and deliver the cold coolant from the chiller towards each component in the system. After cooling the components, the individual lines converge into a return manifold to be brought back into the chiller to dissipate the heat and lower the coolant temperature through the refrigeration circuit. Orifices are placed at the auxiliary, battery, brakes and transmission heat exchanger lines. The primary purpose of the control orifices was to control and direct the flow towards each component depending on their thermal dissipation requirements. As stated previously, the motor will generate the highest heat generation rate of 32 kW during its peak performance, which will happen when the truck was fully loaded and required to move up an incline from a standstill. Therefore, no control orifices are placed in the drive motor lines since it will require the highest coolant flow rate achievable to dissipate the generated heat effectively and efficiently. The remaining control orifices must be configured to open at a certain percentage to direct most of the flow toward the drive motor and inverters without compromising the coolant performance on the other lines.

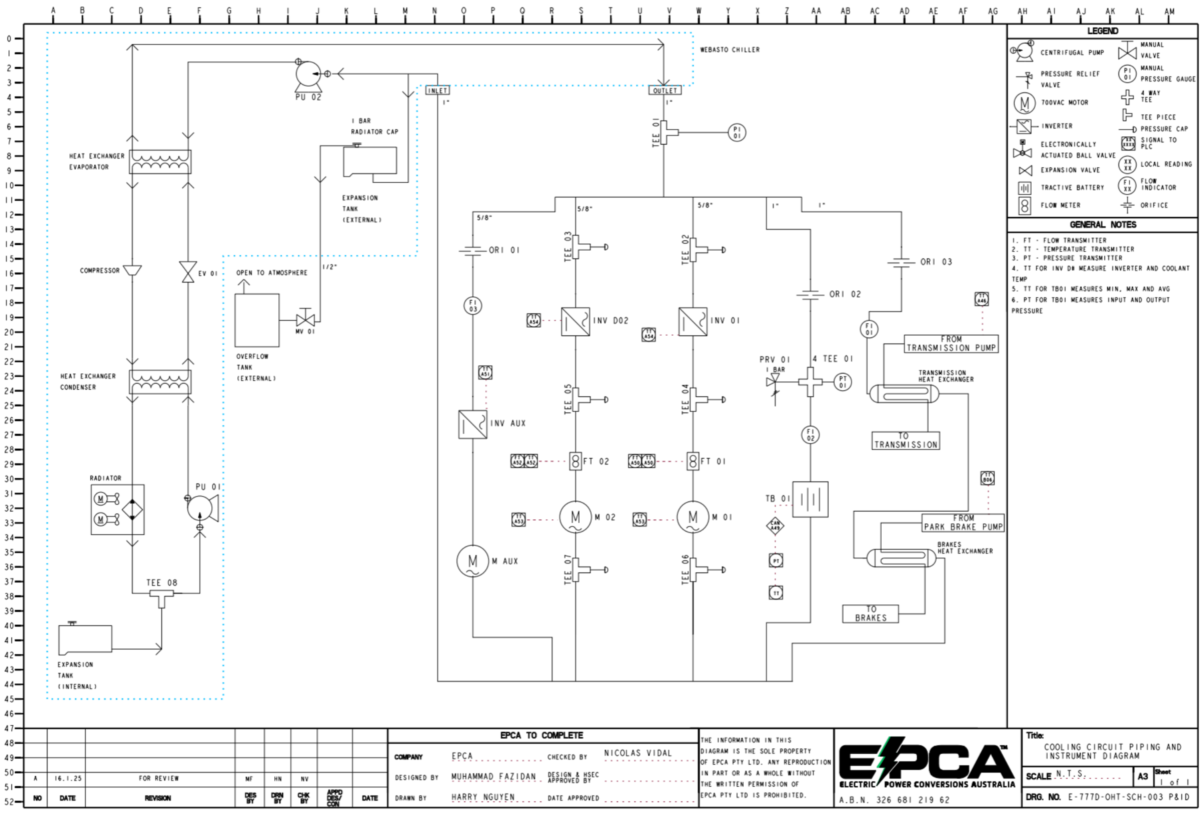

Figure 2: Piping and Instrumentation Diagram

The preliminary digital twin simulation model of the vehicle was shown in Figure. 3.

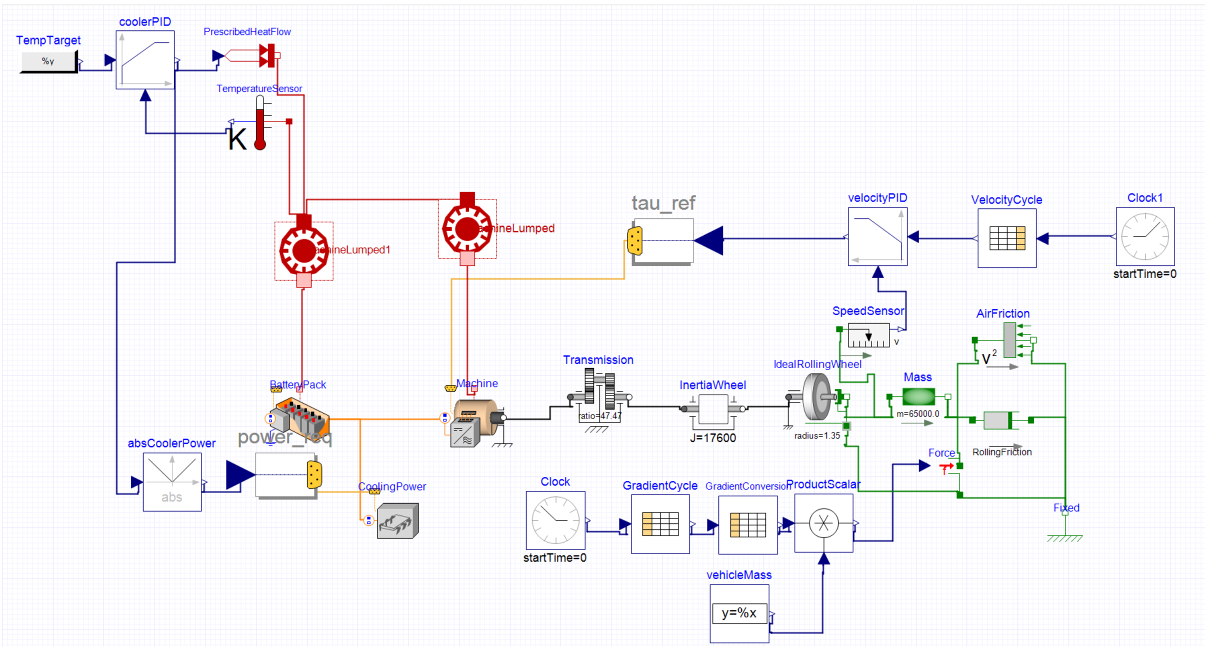

Figure 3: Digital Twin Model of EPCA 100T Electric Truck

The ANSYS Twin Builder Software has enabled our team to create a comprehensive digital twin of the vehicle's system, allowing us to accurately predict its behaviour under various operating conditions by inputting key parameters such as the velocity profile. This digital twin encompasses all major components of the vehicle, including the battery pack, main drive motor, transmission, and wheels.

In this model, the battery was represented as a single cell, with critical characteristics like open circuit voltage, state of charge, and impedance precisely defined. These cells are arranged in a 2D array to simulate the six battery packs in the vehicle. The main drive motor was modelled with distinct electrical and mechanical characteristics: it acts as a current source on the electrical side and as a torque source on the mechanical side. The relationship between these aspects was governed by an efficiency map that covers both the motor and its controller, ensuring an accurate simulation of energy conversion and losses.

The transmission was modelled as a fixed ratio system that links the motor shaft to the wheel shaft, assuming no losses in the process. The wheels are defined by their radius and rotational inertia, with the interaction between the wheels and the road surface modelled under the assumption of a non-slip condition, ensuring a realistic depiction of vehicle dynamics.

For thermal management, the chiller component in the model simulates a controllable heat flow, either into or out of the system. The thermal loads within the system are the cumulative result of losses from the converter, motor, and battery pack. To maintain optimal operating conditions, a temperature target of 35°C was set, and a PID loop dynamically regulates the heat flow to achieve this target. The controller was designed to manage maximum cooling and heating capacities in accordance with the specifications provided in the datasheet, ensuring that the system remains within safe thermal limits during operation.

Please refer to Appendix 2 for the ANSYS simulation report.

2.2. Manufacturing and Installation of System

The project's second stage was the manufacturing and installation of the cooling system onto the truck. The chiller system was placed on top of the battery, utilising the existing mounting locations for efficient integration into the Caterpillar 777D vehicle. A chiller mount was designed and manufactured to suit the chiller's mounting requirements and the rigorous operating conditions, such as high vibration in a mining site.

Figure 4: Chiller BTMS Unit

Figure 4 displays the Webasto BTMS unit installed on the 777D vehicle. Note that the chiller was placed on top of the battery compartment to ensure efficient airflow to the air blast system in the chiller from the higher elevation.

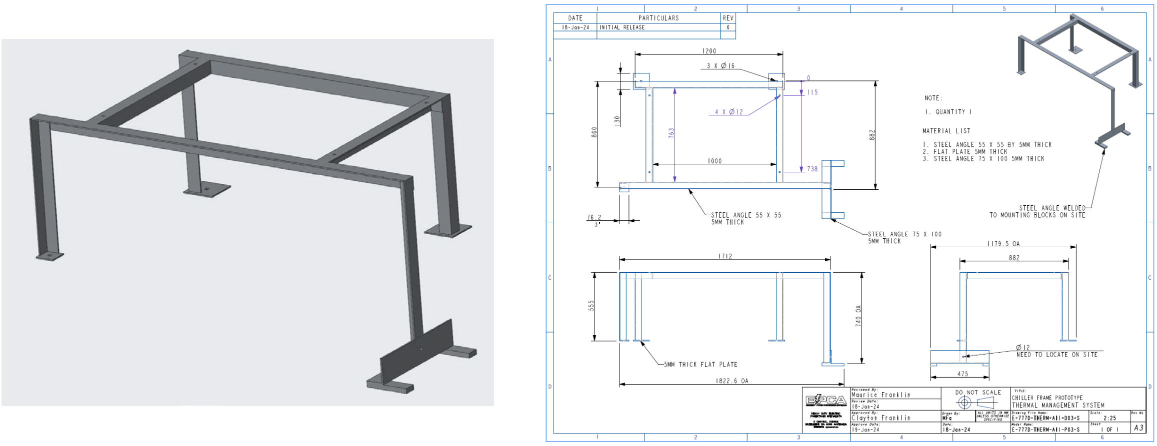

Figure 5: CAD Model and Technical Drawing of the BTMS Frame.

Figure 5 displays the CAD model and the drawing of the chiller frame mount. The chiller frame was designed and manufactured to suit the Webasto chiller. Moreover, the modular design of the BTMS chiller allows it to be interchangeable with different chiller models or brands because the mounting points will remain the same. The only required changes are modifications to the lateral brace to allow for the mounting of chiller units of different sizes.

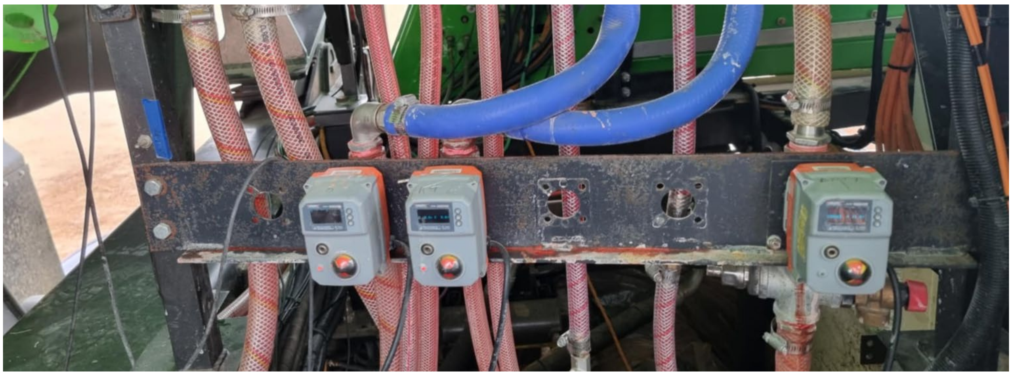

Figure 6: Flow Orifices

Figure 6 showed the orifices that controls the flow rate to each component in the system. The manifold was a single unit separated into two sections by a separator plate. One section acts as the common header that distributes the chiller's coolant to all the components, while the other section acts as a return header from all the components back to the chiller. The orifices are mounted on separate sheet metal mounts at the output of the chiller. Tests are done to determine the ideal opening percentages to reflect the required cooling capacity for each component.

Figure 7: Cooling System Header Tank

Figure 7 displays the header tank of the cooling circuit. The header tank was connected directly to the chiller's expansion tank through a radiator cap. Similar to a typical car radiator system, in the event that the pressure in the cooling circuit increases, the expansion will vent the coolant out to the header tank. Conversely, if the coolant reduces in temperature and pressure, it will create a vacuum, which in turn will draw the required excess coolant from the header tank.

2.3. Control Systems and Coding Development

Vehicle Control Unit Code

The chiller was mainly run and controlled through a program called Thermal Management (PRG). This program was then controlled by the master program vehicle (PRG) which alters the state of the device by using functions and variables present Thermal Management program. Figure 8 showed an overview list of cooling system programs and functions that run on the vehicle control unit.

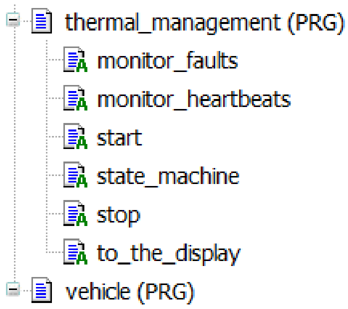

Figure 8: Chiller Code Overview

The Thermal Management program handles all functionality regarding the chiller. The programs and functions do the following (See table 4):

Table 3: Thermal Management Programs/Functions

Program/Function	**Description of Functionality**
Thermal management (PRG)	The main program that declares all the variables and runs monitor_faults, monitor_heartbeats, state_machine and to_the_display sub functions.
Monitor_faults	Monitors the faults sent out by the chiller.
Monitor_heartbeats	Monitors the heartbeat of the chiller via CANBUS.
Start	Sets the Startup variable to true which alters the state_machine function.
State_machine	Controls the state of the chiller. The chiller has 3 states: • Standby: Default mode chiller starts during Low voltage, and waits for the startup signal before moving to the next state. • Request_Mode: Sets the temperature setpoint and enables flags on the chiller to allow the chiller

	to begin cooling. Once done it signals that it is ready for the vehicle to run. Will go to powerdown state if a stop command is received or a fault has occurred. • Powerdown: This state shuts down the chiller and returns it to the standby state.
Stop	Sets the stop variable to true which alters the state_machine function.
To_the_display	Sends data from the Vehicle Control Unit to the HMI for display and logging.

The code was written in a mixture of Structured Text and Function Blocks. Below was the main program of the state machine function for the thermal management program. The below figure showed the standby state in which the devices wait until the startup signal was given. When given the signal it will move onto the next state.

The next state was Request Mode where first it checks the chiller for any errors or a signal to stop and shut down the system, if no signal was received, it proceeds to perform normally. If there was a signal for manual control from the HMI display the values from said display will override the defaults. If no signal was given, the VCU chooses the default temperature set point to 20 degrees and enables the heating and cooling flag.

Once the chiller was running, it will then set the ready-to-start flag to true to indicate to the main vehicle program that the system was running and ready to begin truck operation. If a stop signal was activated, it will set the thermal state to the powered down state. This state will start the process of turning off the chiller, it will disable the cooling and heating flag and wait for the chiller to enter its standby mode before eventually setting the signal that it was ready to turn off.

thermal_management.state_machine

```
IF stop_system = 1 THEN
    thermal_state := POWERDOWN;
END_IF

CASE thermal_state OF

    //Wait until batteries are ready
    //Wait in LV unitl startup signal is given
    STANDBY:
        IF startup = 1 THEN

            TMS1_ThermSysStrtReq1_1939 := 1;
            thermal_state := REQUEST_MODE;

        END_IF

    //Normal Operational mode
    REQUEST_MODE:

        //Checks for errors from chiller or is told to stop
        IF TMS1_eBTM_ECU_Error THEN

            //Communicates error to the vehicle control state
            vehicle.monitor_faults(faulted_system_number := constants.CHILLER1_FAULT_CODE, shutdown_type := constants.normal_shutdown);
            thermal_state := POWERDOWN;

        ELSIF stop_system = 1 THEN
            thermal_state := POWERDOWN;

        ELSIF TMS1_ThermMngtSysMode_J1939 = 14 AND ready_to_start = TRUE THEN
            vehicle.monitor_faults(faulted_system_number := constants.CHILLER1_FAULT_CODE, shutdown_type := constants.normal_shutdown);
            thermal_state := POWERDOWN;

        //Normal Operation
        ELSE

            //Manual Control Signal
            IF display_to_vcu.chillers_enable_manual_control THEN
                IF display_to_vcu.chillers_enable_tsetpoint THEN
                    TMS1_TSetPoint_J1939 := display_to_vcu.chillers_tsetpoint;
                    //Double Check, should be guarded at input
                    IF TMS1_TSetPoint_J1939 < 0 THEN
                        TMS1_TSetPoint_J1939 := 0;
                    ELSIF TMS1_TSetPoint_J1939 > 35 THEN
                        TMS1_TSetPoint_J1939 := 35;
                    END_IF

                    TMS1_EnaCoolgHeatgBatFlag_J1939 := 1;
                ELSE
                    TMS1_EnaCoolgHeatgBatFlag_J1939 := 0;
                END_IF
            ELSE
```

Figure 9: State Machine of Thermal Management Program Image 1

thermal_management.state_machine

```
            thermal_state := POWERDOWN;

        ELSIF stop_system = 1 THEN
            thermal_state := POWERDOWN;

        ELSIF TMS1_ThermMngtSysMode_J1939 = 14 AND ready_to_start = TRUE THEN
            vehicle.monitor_faults(faulted_system_number := constants.CHILLER1_FAULT_CODE, shutdown_type := constants.normal_shutdown);
            thermal_state := POWERDOWN;

        //Normal Operation
        ELSE

            //Manual Control Signal
            IF display_to_vcu.chillers_enable_manual_control THEN
                IF display_to_vcu.chillers_enable_tsetpoint THEN
                    TMS1_TSetPoint_J1939 := display_to_vcu.chillers_tsetpoint;
                    //Double Check, should be guarded at input
                    IF TMS1_TSetPoint_J1939 < 0 THEN
                        TMS1_TSetPoint_J1939 := 0;
                    ELSIF TMS1_TSetPoint_J1939 > 35 THEN
                        TMS1_TSetPoint_J1939 := 35;
                    END_IF

                    TMS1_EnaCoolgHeatgBatFlag_J1939 := 1;
                ELSE
                    TMS1_EnaCoolgHeatgBatFlag_J1939 := 0;
                END_IF
            ELSE
                //Normal Operation
                TMS1_TSetPoint_J1939 := 20;
                TMS1_EnaCoolgHeatgBatFlag_J1939 := 1;

                //Signal that they are ready to start
                IF TMS1_ThermMngtSysMode_J1939 > 0 AND TMS1_ThermMngtSysMode_J1939 < 4 THEN
                    ready_to_start := TRUE;
                END_IF
            END_IF

        END_IF

    POWERDOWN:

        //Disable Cooling
        TMS1_EnaCoolgHeatgBatFlag_J1939 := 0;

        //Tell Vehicle that system is ready to turn off
        IF TMS1_ThermMngtSysHv_J1939 < 10 THEN
            ready_to_turn_off := TRUE;
        END_IF

END_CASE
```

Figure 10: State machine of Thermal Management Program Image 2

The communication between the chiller and VCU was done by CANBUS utilising J1939 CANBUS protocol. Figure 11 showed the two Electronic Control Units (ECU) that deal with translating and managing the CANBUS data being sent to the chiller and from the chiller.

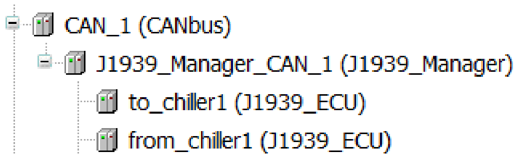

Figure 11: CANBUS Chiller Units

Each ECU contains a list of signals that it expects to receive and send onto the CANBUS line. Figure 12 showed a portion of signals received from the chiller. A variety of information from the chiller can be obtained such as its status or if the high voltage bus was under or over voltage. The information was then mapped to an address and given a variable name with size allocated for each signal determined by the type of the data.

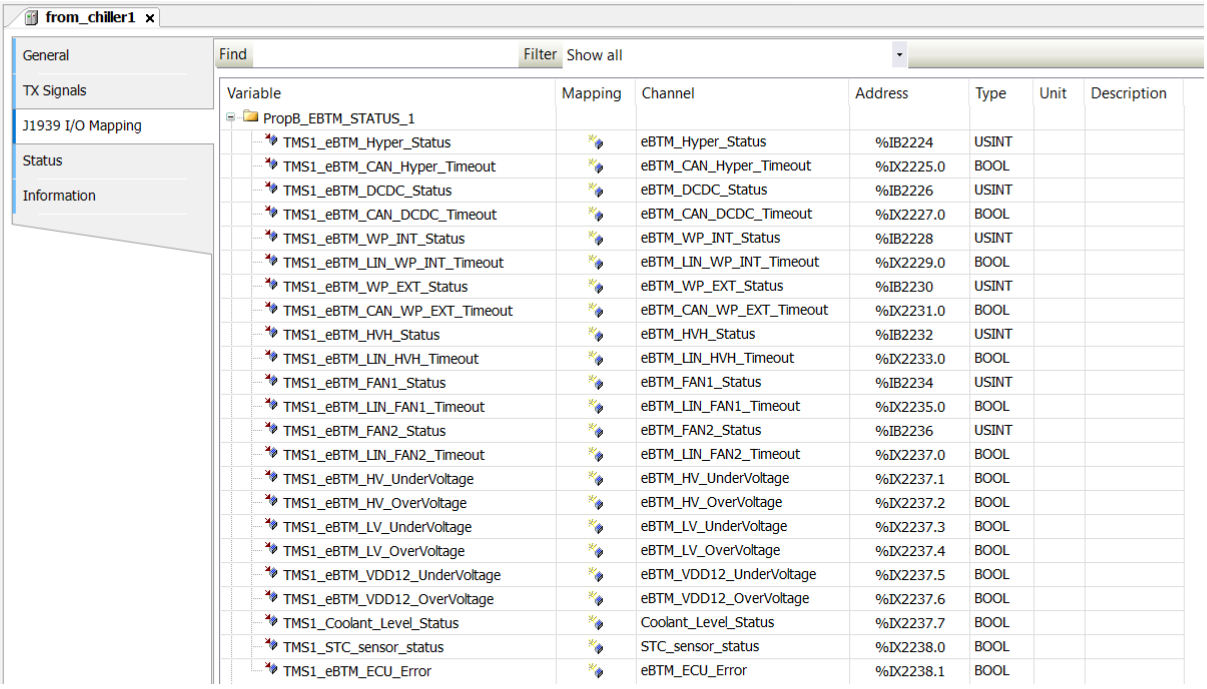

Variable	Mapping	Channel	Address	Type	Unit	Description
PropB_EBTM_STATUS_1						
TMS1_eBTM_Hyper_Status		eBTM_Hyper_Status	%IB2224	USINT		
TMS1_eBTM_CAN_Hyper_Timeout		eBTM_CAN_Hyper_Timeout	%IX2225.0	BOOL		
TMS1_eBTM_DCDC_Status		eBTM_DCDC_Status	%IB2226	USINT		
TMS1_eBTM_CAN_DCDC_Timeout		eBTM_CAN_DCDC_Timeout	%IX2227.0	BOOL		
TMS1_eBTM_WP_INT_Status		eBTM_WP_INT_Status	%IB2228	USINT		
TMS1_eBTM_LIN_WP_INT_Timeout		eBTM_LIN_WP_INT_Timeout	%IX2229.0	BOOL		
TMS1_eBTM_WP_EXT_Status		eBTM_WP_EXT_Status	%IB2230	USINT		
TMS1_eBTM_CAN_WP_EXT_Timeout		eBTM_CAN_WP_EXT_Timeout	%IX2231.0	BOOL		
TMS1_eBTM_HVH_Status		eBTM_HVH_Status	%IB2232	USINT		
TMS1_eBTM_LIN_HVH_Timeout		eBTM_LIN_HVH_Timeout	%IX2233.0	BOOL		
TMS1_eBTM_FAN1_Status		eBTM_FAN1_Status	%IB2234	USINT		
TMS1_eBTM_LIN_FAN1_Timeout		eBTM_LIN_FAN1_Timeout	%IX2235.0	BOOL		
TMS1_eBTM_FAN2_Status		eBTM_FAN2_Status	%IB2236	USINT		
TMS1_eBTM_LIN_FAN2_Timeout		eBTM_LIN_FAN2_Timeout	%IX2237.0	BOOL		
TMS1_eBTM_HV_UnderVoltage		eBTM_HV_UnderVoltage	%IX2237.1	BOOL		
TMS1_eBTM_HV_OverVoltage		eBTM_HV_OverVoltage	%IX2237.2	BOOL		
TMS1_eBTM_LV_UnderVoltage		eBTM_LV_UnderVoltage	%IX2237.3	BOOL		
TMS1_eBTM_LV_OverVoltage		eBTM_LV_OverVoltage	%IX2237.4	BOOL		
TMS1_eBTM_VDD12_UnderVoltage		eBTM_VDD12_UnderVoltage	%IX2237.5	BOOL		
TMS1_eBTM_VDD12_OverVoltage		eBTM_VDD12_OverVoltage	%IX2237.6	BOOL		
TMS1_Coolant_Level_Status		Coolant_Level_Status	%IX2237.7	BOOL		
TMS1_STC_sensor_status		STC_sensor_status	%IX2238.0	BOOL		
TMS1_eBTM_ECU_Error		eBTM_ECU_Error	%IX2238.1	BOOL		

Figure 12: Chiller CAN Signals Configuration

HMI Display Code

The HMI displays data via its screen for the user to monitor and control elements if required. Figure 13 showed the setup for such a screen. The screen was split into two sections, the data from the chiller and temperature from other devices. Note the screen has been designed for multiple chillers and batteries but not all of them are implemented on the current truck, any non-implemented value will have the value %d.

The chiller section displays the temperature of the coolant, the current temperature setpoint and if such a setpoint causes the chiller to heat or cool the system, power consumption, valid coolant level and if the system has faulted. The temperature setpoint can also be changed here if desired. The temperature section showed the temperature of the batteries, both drive inverters and auxiliary.

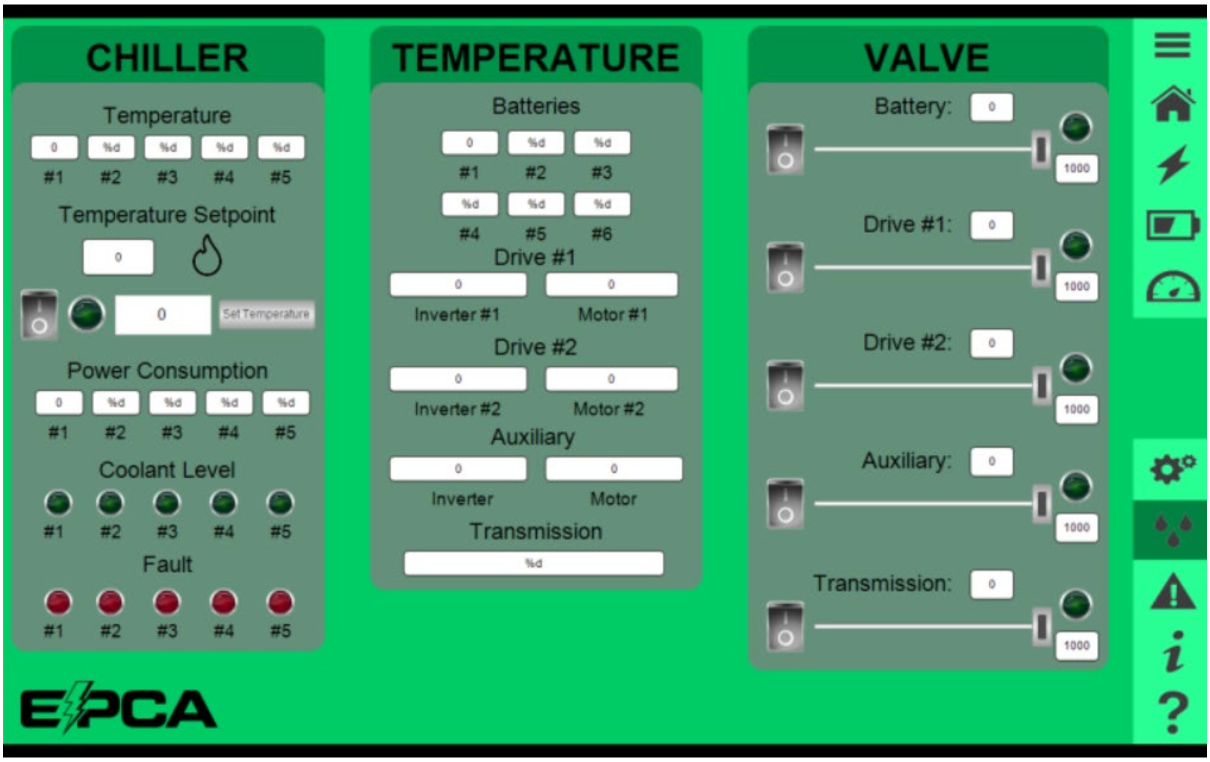

Figure 13: HMI Chiller Screen during Simulation

The HMI also runs code to maintain elements of the screen and to log the data from the chiller onto a USB. The Figure 14 and 15 show the overview of the structure of the logging code as well as the section that deals with the chiller screen.

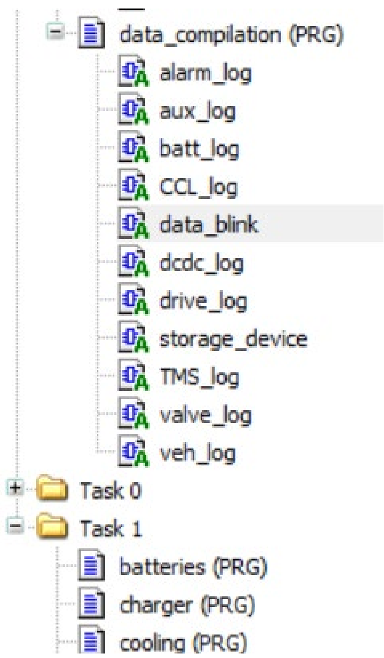

Figure 14: HMI Chiller and Logging Code

The following are the important functions and programs regarding the chiller screen and logging code (See Table 5):

Table 4: HMI Chiller and Logging Programs/Functions

Program/Function	**Description of Functionality**
Data_compliation (PRG)	The main program runs and compiles the data received from the vehicle control unit and puts it into the correct format for storage on the USB. It first verifies that the USB connection is established and creates the files and format for logging. It then compiles the data for logging. It also runs the sub-functions Data_Blink, Storage_device and TMS_log.
Data_blink	Controls timing for saving data onto the USB.
Storage_device	Deals with the connection of the USB to the HMI and allows for safe disconnection of the USB from the HMI.
TMS_log	Deals with writing the TMS data onto the USB in CSV format. Records two separate files, one for data being sent to the chiller from the vehicle control unit and one being data from the chiller unit. The data is time-stamped when the recording started.
Cooling (PRG)	Deals with the chiller screen logic for displaying and altering variables based on user input such as the temperature setpoint.

The data being logged by the HMI was currently taken every second and logs that value are sent out from and to the chiller. Figure 15 showed how the HMI formats the chiller data. It does this by creating a long CSV string. It first converts the data into a string with a separator. It then concatenates the string repeatedly with different points of data. This was also repeated separately for data sent to the chiller.

```
    // Chiller
    TMS1_Data := ifmFileUtil.ANY_TYPE_TO_STRING(vcu_to_display.TMS_eBTM_Hyper_Status[0],seperator);
    TMS1_Data := ifmFileUtil.ifmCONCAT(TMS1_Data, ifmFileUtil.ANY_TYPE_TO_STRING(vcu_to_display.TMS_eBTM_CAN_Hyper_Timeout[0],seperator));
    TMS1_Data := ifmFileUtil.ifmCONCAT(TMS1_Data, ifmFileUtil.ANY_TYPE_TO_STRING(vcu_to_display.TMS_eBTM_DCDC_Status[0],seperator));
    TMS1_Data := ifmFileUtil.ifmCONCAT(TMS1_Data, ifmFileUtil.ANY_TYPE_TO_STRING(vcu_to_display.TMS_eBTM_CAN_DCDC_Timeout[0],seperator));
    TMS1_Data := ifmFileUtil.ifmCONCAT(TMS1_Data, ifmFileUtil.ANY_TYPE_TO_STRING(vcu_to_display.TMS_eBTM_WP_INT_Status[0],seperator));
    TMS1_Data := ifmFileUtil.ifmCONCAT(TMS1_Data, ifmFileUtil.ANY_TYPE_TO_STRING(vcu_to_display.TMS_eBTM_LIN_WP_INT_Timeout[0],seperator));
    TMS1_Data := ifmFileUtil.ifmCONCAT(TMS1_Data, ifmFileUtil.ANY_TYPE_TO_STRING(vcu_to_display.TMS_eBTM_WP_EXT_Status[0],seperator));
    TMS1_Data := ifmFileUtil.ifmCONCAT(TMS1_Data, ifmFileUtil.ANY_TYPE_TO_STRING(vcu_to_display.TMS_eBTM_CAN_WP_EXT_Timeout[0],seperator));
    TMS1_Data := ifmFileUtil.ifmCONCAT(TMS1_Data, ifmFileUtil.ANY_TYPE_TO_STRING(vcu_to_display.TMS_eBTM_HVH_Status[0],seperator));
    TMS1_Data := ifmFileUtil.ifmCONCAT(TMS1_Data, ifmFileUtil.ANY_TYPE_TO_STRING(vcu_to_display.TMS_eBTM_LIN_HVH_Timeout[0],seperator));
    TMS1_Data := ifmFileUtil.ifmCONCAT(TMS1_Data, ifmFileUtil.ANY_TYPE_TO_STRING(vcu_to_display.TMS_eBTM_FAN1_Status[0],seperator));
    TMS1_Data := ifmFileUtil.ifmCONCAT(TMS1_Data, ifmFileUtil.ANY_TYPE_TO_STRING(vcu_to_display.TMS_eBTM_LIN_FAN1_Timeout[0],seperator));
    TMS1_Data := ifmFileUtil.ifmCONCAT(TMS1_Data, ifmFileUtil.ANY_TYPE_TO_STRING(vcu_to_display.TMS_eBTM_FAN2_Status[0],seperator));
    TMS1_Data := ifmFileUtil.ifmCONCAT(TMS1_Data, ifmFileUtil.ANY_TYPE_TO_STRING(vcu_to_display.TMS_eBTM_LIN_FAN2_Timeout[0],seperator));
    TMS1_Data := ifmFileUtil.ifmCONCAT(TMS1_Data, ifmFileUtil.ANY_TYPE_TO_STRING(vcu_to_display.TMS_eBTM_HV_UnderVoltage[0],seperator));
    TMS1_Data := ifmFileUtil.ifmCONCAT(TMS1_Data, ifmFileUtil.ANY_TYPE_TO_STRING(vcu_to_display.TMS_eBTM_HV_OverVoltage[0],seperator));
    TMS1_Data := ifmFileUtil.ifmCONCAT(TMS1_Data, ifmFileUtil.ANY_TYPE_TO_STRING(vcu_to_display.TMS_eBTM_LV_UnderVoltage[0],seperator));
    TMS1_Data := ifmFileUtil.ifmCONCAT(TMS1_Data, ifmFileUtil.ANY_TYPE_TO_STRING(vcu_to_display.TMS_eBTM_LV_OverVoltage[0],seperator));
    TMS1_Data := ifmFileUtil.ifmCONCAT(TMS1_Data, ifmFileUtil.ANY_TYPE_TO_STRING(vcu_to_display.TMS_eBTM_VDD12_UnderVoltage[0],seperator));
    TMS1_Data := ifmFileUtil.ifmCONCAT(TMS1_Data, ifmFileUtil.ANY_TYPE_TO_STRING(vcu_to_display.TMS_eBTM_VDD12_OverVoltage[0],seperator));
    TMS1_Data := ifmFileUtil.ifmCONCAT(TMS1_Data, ifmFileUtil.ANY_TYPE_TO_STRING(vcu_to_display.TMS_Coolant_Level_Status[0],seperator));
    TMS1_Data := ifmFileUtil.ifmCONCAT(TMS1_Data, ifmFileUtil.ANY_TYPE_TO_STRING(vcu_to_display.TMS_STC_sensor_status[0],seperator));
    TMS1_Data := ifmFileUtil.ifmCONCAT(TMS1_Data, ifmFileUtil.ANY_TYPE_TO_STRING(vcu_to_display.TMS_eBTM_ECU_Error[0],seperator));
    TMS1_Data := ifmFileUtil.ifmCONCAT(TMS1_Data, ifmFileUtil.ANY_TYPE_TO_STRING(vcu_to_display.TMS_EBTM_STM[0],seperator));
    TMS1_Data := ifmFileUtil.ifmCONCAT(TMS1_Data, ifmFileUtil.ANY_TYPE_TO_STRING(vcu_to_display.TMS_DETECTED_CONFIGURATION[0],seperator));
    TMS1_Data := ifmFileUtil.ifmCONCAT(TMS1_Data, ifmFileUtil.ANY_TYPE_TO_STRING(vcu_to_display.TMS_COOLING_AVAILBLE[0],seperator));
    TMS1_Data := ifmFileUtil.ifmCONCAT(TMS1_Data, ifmFileUtil.ANY_TYPE_TO_STRING(vcu_to_display.TMS_HEATING_AVAILBLE[0],seperator));
    TMS1_Data := ifmFileUtil.ifmCONCAT(TMS1_Data, ifmFileUtil.ANY_TYPE_TO_STRING(vcu_to_display.TMS_DETECTED_CAN_PROTOCOL[0],seperator));
    TMS1_Data := ifmFileUtil.ifmCONCAT(TMS1_Data, ifmFileUtil.ANY_TYPE_TO_STRING(vcu_to_display.TMS_FAN_1_SPEED[0],seperator));
    TMS1_Data := ifmFileUtil.ifmCONCAT(TMS1_Data, ifmFileUtil.ANY_TYPE_TO_STRING(vcu_to_display.TMS_FAN_2_SPEED[0],seperator));
    TMS1_Data := ifmFileUtil.ifmCONCAT(TMS1_Data, ifmFileUtil.ANY_TYPE_TO_STRING(vcu_to_display.TMS_PUMP_EXTERNAL_SPEED[0],seperator));
    TMS1_Data := ifmFileUtil.ifmCONCAT(TMS1_Data, ifmFileUtil.ANY_TYPE_TO_STRING(vcu_to_display.TMS_PUMP_INTERNAL_SPEED[0],seperator));
    TMS1_Data := ifmFileUtil.ifmCONCAT(TMS1_Data, ifmFileUtil.ANY_TYPE_TO_STRING(vcu_to_display.TMS_COOLANT_TEMP[0],seperator));
    TMS1_Data := ifmFileUtil.ifmCONCAT(TMS1_Data, ifmFileUtil.ANY_TYPE_TO_STRING(vcu_to_display.TMS_POWER_CONS_HVH[0],seperator));
    TMS1_Data := ifmFileUtil.ifmCONCAT(TMS1_Data, ifmFileUtil.ANY_TYPE_TO_STRING(vcu_to_display.TMS_POWER_CONS_HYPER[0],seperator));
    TMS1_Data := ifmFileUtil.ifmCONCAT(TMS1_Data, ifmFileUtil.ANY_TYPE_TO_STRING(vcu_to_display.TMS_POWER_LIMIT_CALC[0],seperator));
    TMS1_Data := ifmFileUtil.ifmCONCAT(TMS1_Data, ifmFileUtil.ANY_TYPE_TO_STRING(vcu_to_display.TMS_ThermMngtSysSLIInpPwr_J1939[0],seperator));
    TMS1_Data := ifmFileUtil.ifmCONCAT(TMS1_Data, ifmFileUtil.ANY_TYPE_TO_STRING(vcu_to_display.TMS_ThermMngtSysHv_J1939[0],seperator));
    TMS1_Data := ifmFileUtil.ifmCONCAT(TMS1_Data, ifmFileUtil.ANY_TYPE_TO_STRING(vcu_to_display.TMS_ThermMngtSysCmpr_J1939[0],seperator));
    TMS1_Data := ifmFileUtil.ifmCONCAT(TMS1_Data, ifmFileUtil.ANY_TYPE_TO_STRING(vcu_to_display.TMS_ThermMngtSysRel_J1939[0],seperator));
    TMS1_Data := ifmFileUtil.ifmCONCAT(TMS1_Data, ifmFileUtil.ANY_TYPE_TO_STRING(vcu_to_display.TMS_ThermMngtSysHeatrSts_J1939[0],seperator));
    TMS1_Data := ifmFileUtil.ifmCONCAT(TMS1_Data, ifmFileUtil.ANY_TYPE_TO_STRING(vcu_to_display.TMS_ThermMngtSysHVILSts_J1939[0],seperator));
    TMS1_Data := ifmFileUtil.ifmCONCAT(TMS1_Data, ifmFileUtil.ANY_TYPE_TO_STRING(vcu_to_display.TMS_ThermMngtSysMode_J1939[0],seperator));
    TMS1_Data := ifmFileUtil.ifmCONCAT(TMS1_Data, ifmFileUtil.ANY_TYPE_TO_STRING(vcu_to_display.TMS_ThermMngtSysCooltLvl_J1939[0],seperator));

    TMS1_Input_Data := ifmFileUtil.ANY_TYPE_TO_STRING(vcu_to_display.TMS_ThermSYsStrtReql_1939[0],seperator);
    TMS1_Input_Data := ifmFileUtil.ifmCONCAT(TMS1_Input_Data, ifmFileUtil.ANY_TYPE_TO_STRING(vcu_to_display.TMS_PackNameThermReql_J1939[0],seperator));
    TMS1_Input_Data := ifmFileUtil.ifmCONCAT(TMS1_Input_Data, ifmFileUtil.ANY_TYPE_TO_STRING(vcu_to_display.TMS_EnaCoolgHeatgBatFlag_J1939[0],seperator));
```

Figure 15: HMI Code Combining Data Points

Figure 16 showed how the data was formatted when opened by Excel. As shown in the figure you can see the name of the data being recorded and the time and date for when the piece of data was recorded.

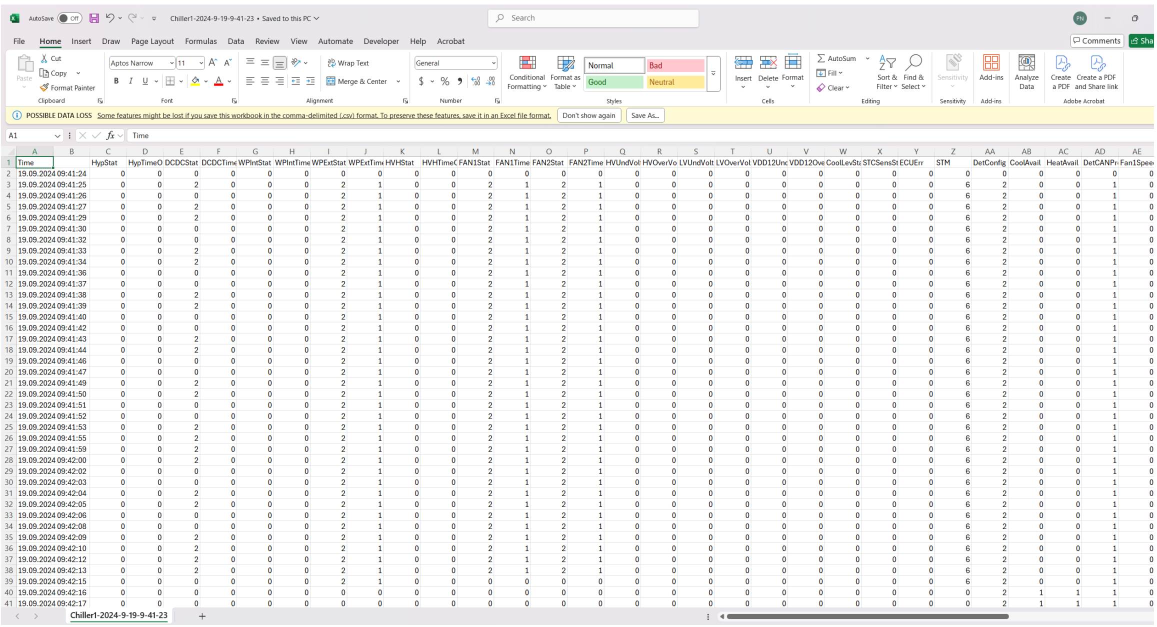

Figure 16: Chiller Logged Data Example

The data that was recorded was saved onto a USB with the following file structure as shown in Figure 17. The HMI first creates a folder with the current date and time. The HMI then creates individual files to store data from each device operating on the truck with date and time as well. Each device has two files, one for input recording data to the device and the other for data from the device.

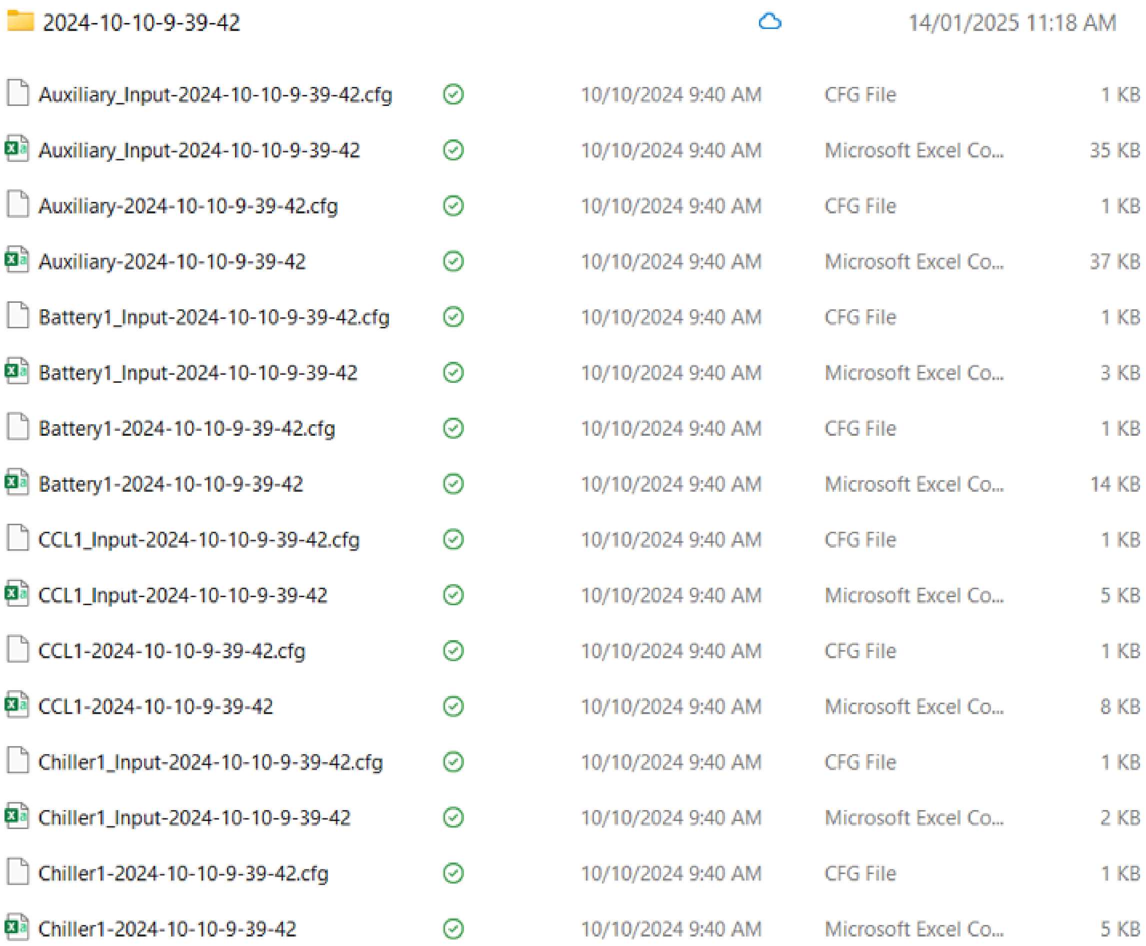

Figure 17: Logging Format Setup on the USB

Wiring Devices

The chiller has been wired up to the low-voltage power and CANBUS. The chiller was wired up to the high-voltage bus located in the PDP. Figures 18, 19, 20, and 21 are images of the devices wired up.

Figure 18: Low Voltage Wiring for Chiller

Figure 19: High Voltage Wiring for the Chiller

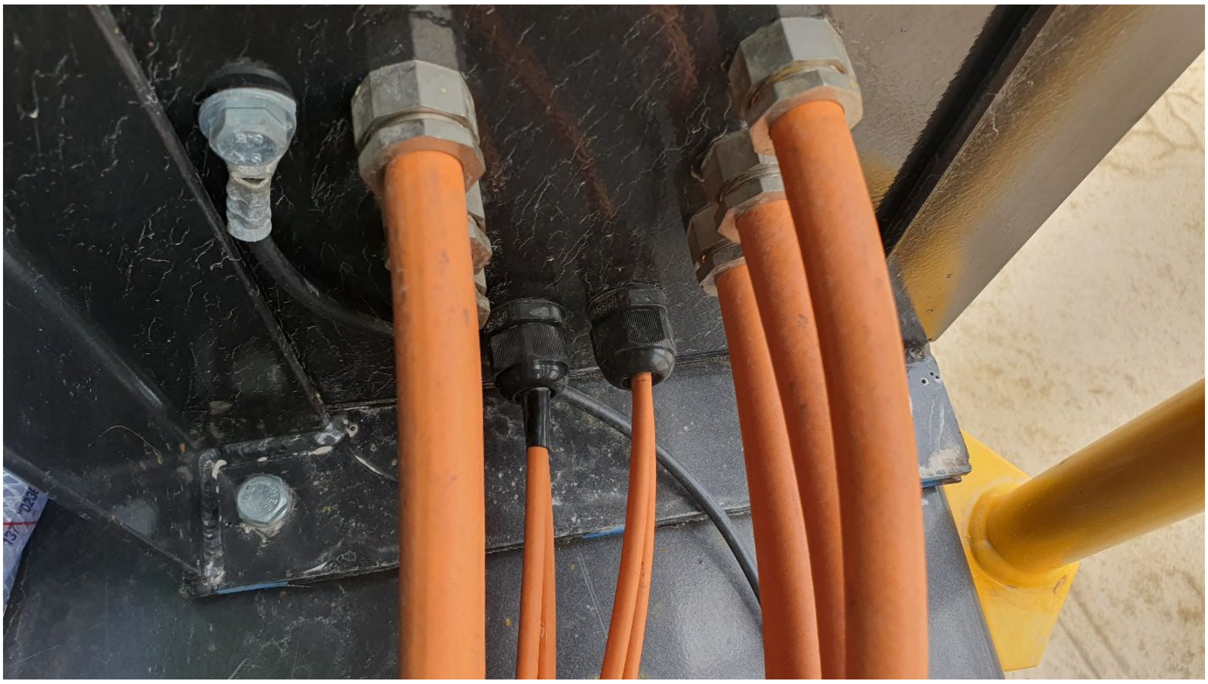

Figure 20: High Voltage Wiring into the PDP

2.4. Cooling System Commissioning and Testing

Once the cooling system has been assembled and coded, the next stage was commissioning it to ensure it operates as intended. The cooling circuit was bled to purge all the air out of the coolant. Testing of the program was done in three ways, one by simulation purely on Codesys, the other in debug mode on actual hardware on the truck and the other via real-world running the program normally on the truck. The first method, Codesys simulation allows for quick testing of programs and functions to ensure the logic works as expected, variables can be altered to allow for quick and easy testing of functions. Figure 22 showed the data_blink function while in simulation mode.

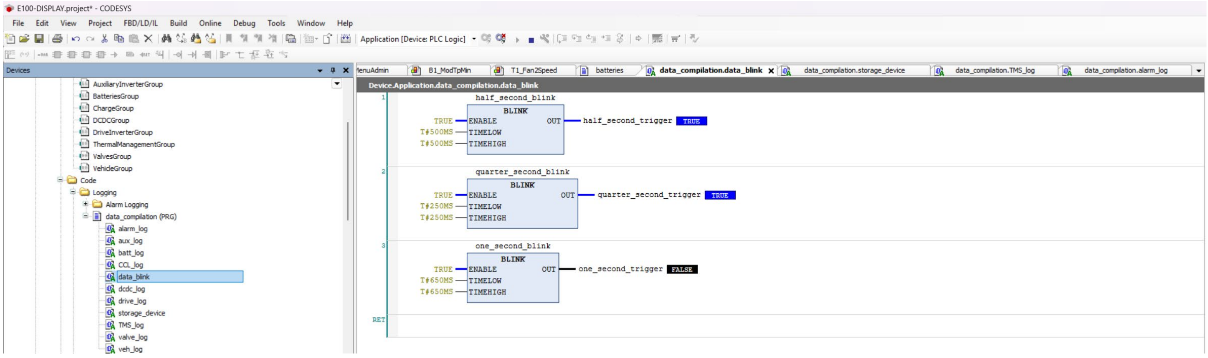

Figure 21: Simulation Mode Data Blink Testing

The second method allows for testing the code on actual hardware whilst allowing the user to monitor the code directly. This allows for testing of the CANBUS communication between the devices, the logic of the code correctly executes etc. Any errors or faults present during this method can then be readily fixed and re-ran again to ensure correct operation.

The last method makes sure that the code can last a long period without any errors or issues. This was important as the two previous methods only look at the code in an isolated and controlled environment. This last section allows for checking of potential oversights and issues that might not be apparent such as unforeseen inter-device interactions.

Once the code has been tested, the truck was ready to be load tested on the site, as outlined in the following sections.

3. Results and Findings

After completing the vehicle's commissioning stage, the truck was transported to a sand pit mine site at Bakers Hill for rigorous load testing. This stage was crucial for the engineering design team to gather the relevant data, develop a better understanding of the truck's cooling system, identify areas of improvement, and develop design improvements for later revisions. The following section details the stages of the results and findings of the vehicle cooling system testing.

3.1. Load Testing in Mining Environment

As stated in the introduction, the power electronics that power and drive the truck have a lower temperature operating range than the internal combustion engine counterpart. The purpose of this load-testing stage in the mining environment was to monitor the performance of the vehicle operating in a mine setting under load at different ambient conditions. Figure 23 displays the EPCA truck being tested at Bakers Hill mine site.

Figure 22: EPCA's E-777D-OHT Truck Being Tested at Bakers Hill

Test 1: Orifice Opening Percentage

Referring to the P&ID in Fig. 1, the cooling lines are equipped with a few orifices to manage the flow rate to each component in the system. The preliminary design states that the drive motor will produce the highest heat generation rate during peak driving. The purpose of this test was to determine the ideal opening percentage of the auxiliary, battery, brakes and transmission heat exchangers to deliver the maximum flow rate towards the drive inverters and motors. The test will take place at a sand pit mine site located at Bakers Hill, 73 km east of Perth.

The procedure to determine the opening of the control orifices:

1. Open all the flow orifices at 100%.

2. Before driving, enable the chiller at a set temperature of 20°C.
3. Operate the chiller until the coolant level reaches a steady state with a fixed temperature of 20°C.
4. Monitor the pressure of the battery to avoid reaching its pressure limit of 1 bar.
5. Drive the truck for one lap at the mine site.
6. Drive the vehicle at the selected mine site consistently across all tests with different orifice opening percentages. Ensure the driving track has an incline to test the peak heat generated by the drive inverters.
7. Log the highest temperature the max inverter reached. Pay close attention to the temperature when driving up an incline.
8. Repeat the test with different orifice opening percentages if the inverter temperature was above the derating temperature of 45°C.

Test 2: Chiller Temperature Validation

The purpose of this test was to validate the coolant temperature reading taken from the chiller. This test will utilise a Fluke device with a temperature probe placed between the barb and hose at the chiller's outlet port.

The procedure to measure the coolant temperature readings at the outlet of the chiller:

1. Install the temperature probe between the barb and hose at the outlet of the chiller.
2. Enable the chiller at a set temperature of 20°C. Recommended to run truck without auxiliary turned on to reduce the amount of heat the chiller needs to reject.
3. Run the system for 5 minutes for a large sample size for validation.
4. Record the coolant temperature readings from the Fluke temperature probe over the test period.
5. Compare the chiller's coolant temperature logged by the HMI with the temperature probe data.

Test 3: Stationary Testing

This test's purpose was to determine the nominal operation of the chiller's pump at a fixed set point temperature. This test should be conducted after test 1 was completed. The test will provide us with the flow rate and pressure characteristics at different points in the circuit.

The procedure to measure the flow rate and the pressure of the cooling system:

1. Enable the chiller at a set temperature of 25°C. Run chiller until the coolant temperature reaches 25ºC to achieve a steady state. Recommended to run truck without auxiliary turned on to reduce the amount of heat the chiller needs to reject.

2. Record the total pressure reading from the pressure gauge indicator PI 01.
3. Record the flow rate reading at FT 01, FT02, FI 01, FI 02, and FI 03. Sum them all up to determine the overall flow rate in the system.
4. Record the pressure reading at Tee 02, Tee 03, Tee 04, Tee 05, Tee 06, and Tee 07.
5. Record the inlet and outlet pressure reading of the battery (TB 01) from the HMI.

Test 4: Drive Inverter and Motor Performance Testing

This test's purpose was to determine the cooling performance of the two drive inverters and motors. This test utilises some of the data measure in the "Stationary Testing" above.

The procedure to determine the cooling performance of the two drive inverters and motors:

1. Pressure data before the inverter, between the inverter and motor, and after the motor has been measured in the previous test. The measurements should be done again to confirm values are accurate.
2. Flow data for both the circuits for the drive inverter and motor for 1 and 2 has already been measured in the previous test. The measurements should be done again to confirm values are accurate.
3. Inverter inlet temperature was recorded by the chiller and logged continuously by the HMI. The inverter also reports the estimated coolant temperature which can be compared to the chiller measurement.
4. Inverter outlet temperature was recorded by flow meters FT 01 and FT 02 and are logged continuously by the HMI.
5. Motor outlet temperature was recorded by the Fluke devices and wirelessly transmitted to a laptop or phone. This was done by inserting the temperature probe between the barb and hose so that the probe contacts the coolant directly. This transmitted data was logged by the receiving device.

3.2. Data Collected via Vehicle Control Unit

After completing the site testing, the testing data was collected through the Vehicle Control Unit (VCU). Figure. 24 displays the group of data collected as a readable.csv file.

- Auxiliary_Input-2024-9-18-13-35-29.csv
- Auxiliary-2024-9-18-13-35-29.csv
- Battery1_Input-2024-9-18-13-35-29.csv
- Battery1-2024-9-18-13-35-29.csv
- ChargeController1-2024-9-18-13-35-29.csv
- Chiller1_Input-2024-9-18-13-35-29.csv
- Chiller1-2024-9-18-13-35-29.csv
- Drive1_Input-2024-9-18-13-35-29.csv
- Drive1-2024-9-18-13-35-29.csv
- Drive2_Input-2024-9-18-13-35-29.csv
- Drive2-2024-9-18-13-35-29.csv
- Vehicle-2024-9-18-13-35-29.csv

Figure 23: Logged Data from Vehicle Testing

The data logger was programmed to output the input and output parameters of a particular system in the vehicle. Figure. 25 displays the transient data input parameter of the chiller, where the research team are mainly concerned with the chiller's temperature set point of 20°C.

Time	ThermSysStrt	PackNameThem	EnaCoolgHeatBat	TAct	TSetPoint
18.09.2024 13:36:31	1	0	1	0	20
18.09.2024 13:36:32	1	0	1	0	20
18.09.2024 13:36:33	1	0	1	0	20
18.09.2024 13:36:34	1	0	1	0	20

Figure 24: Input Parameter Data

Figure. 26 displays the chiller unit's sample output parameters over the drive's duration. The parameter of interest was to know the value of coolant temperature and the compressor power consumption.

Time	Fan1Spee	Fan2Spee	PumpExtSpeed	PumpIntSpeed	CoolTemp	Cmpr	CooltLvl
18.09.2024 13:36:43	60	60	100	70	23	8160	1
18.09.2024 13:36:44	59	59	100	70	23	8160	1
18.09.2024 13:36:45	58	58	100	70	23	8160	1
18.09.2024 13:36:46	64	64	100	70	23	8160	1
18.09.2024 13:36:47	69	69	100	70	23	8160	1

Figure 25: Output Parameter Data

3.3. Data Analysis and Model Verification

Test 1 Results

Table 6 displays the results of the flow orifice opening percentage tested under similar conditions. The test started with all the orifices opened at 100%. The HMI displays a peak inverter temperature of 63°C, especially during the drive up an incline. The test was repeated until the inverter temperature dropped below the first derating temperature. In conclusion, the test stops at an opening percentage of 10% for the heat exchangers, 10% for the auxiliary drive, and 20% for the battery. The new orifice opening percentage results in a max inverter temperature of 43.2°C and a battery max temperature of 36°C. The test was stopped here since the research team have managed to make the inverter temperature below the first derating temperature, and the research team want to avoid further increasing the battery temperature.

Table 5: Orifices Opening Percentage Results

Test No.	Description	Results
1.	Orifices opening percentage: Heat exchangers orifice – 100% Auxiliary drive orifice – 100% Battery orifice – 100%	Inverter maximum temperature – 63.0°C Battery Inlet Pressure – 0.12 Bar Battery max temperature – 33°C
2.	Orifices opening percentage: Heat exchangers orifice –50% Auxiliary drive orifice – 50% Battery orifice – 70%	Inverter maximum temperature – 56.3°C Battery Inlet Pressure – 0.17 Bar Battery max temperature – 34°C
3.	Orifices opening percentage: Heat exchangers orifice – 20% Auxiliary drive orifice – 20% Battery orifice – 25%	Inverter maximum temperature – 47.4°C Battery Inlet Pressure – 0.25 Bar Battery max temperature – 34°C
4.	Orifices opening percentage: Heat exchangers orifice – 10% Auxiliary drive orifice – 10% Battery orifice – 20%	Inverter maximum temperature – 43.2°C Battery Inlet Pressure – 0.31 Bar Battery max temperature – 36°C

Test 2 Results

Figure 27 displays the temperature reading plot of the chiller sensor and the Fluke temperature probe reading. The chiller temperature was set to 20°C for the 5-minute test duration. The result showed that the temperature reading of the chiller remains constant at 20°C while the fluke temperature reading displays a slight discrepancy with an average temperature reading of 20.19°C.

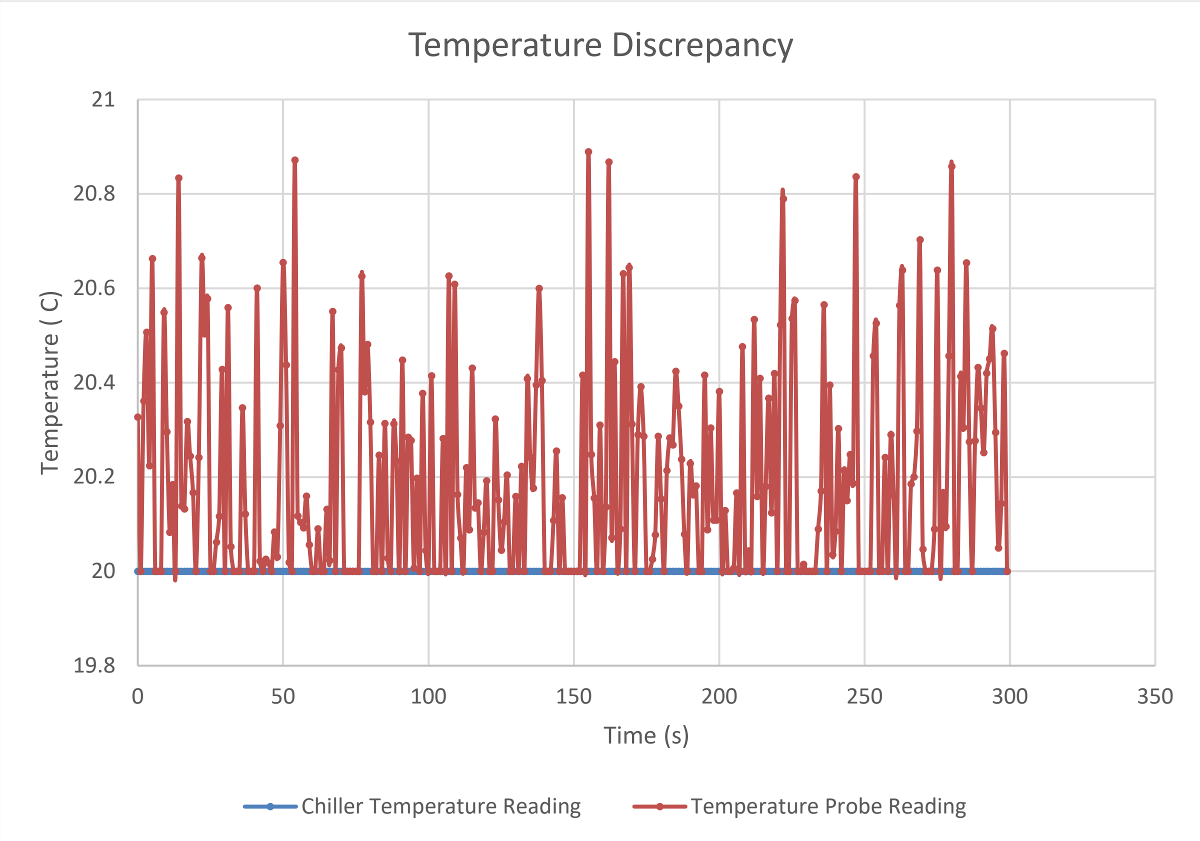

Figure 26: Temperature Discrepancy Reading Between Chiller and Probe

Table 6: Chiller Temperature Validation Reading

Test No.	Description	Results
1.	The chiller was running for 5 minutes, and the temperature reading was recorded from the HMI for the chiller temperature and the Fluke temperature reading from the temperature probe.	Average temperature readings from chiller – 20°C Average temperature readings from Fluke logger – 20.19°C

Test result 3

Table 8 displays the stationary test results that analyse the coolant pressure and volumetric flow rate properties along different points in the lines. The fluid flow properties will give a more detailed insight into the heat dissipation properties of the components in the system.

Table 7: Coolant Fluid Dynamic Properties Result

Test No.	Description	Results
1.	Total Inlet Manifold Pressure	PI 01 – 0.9 Bar
2.	Flow Rate Readings at Each Line	FT 01 – 17 LPM FT 02 – 15 LPM FI 01 – 4 LPM FI 02 – 7 LPM FI 03 – 3 LPM SUM – 46 LPM
3.	Pressure Readings	Tee 02 – 0.40 Bar Tee 03 – 0.43 Bar Tee 04 – 0.32 Bar Tee 05 – 0.36 Bar Tee 06 – 0.08 Bar Tee 07 – 0.1 Bar TB 01 Inlet – 0.03 Bar TB 01 Outlet – 0.01 Bar

Test 4 Results

Figure 28 displays the temperature profile of the coolant inlet temperature from the chiller, drive inverter hotspot temperature, battery average temperature, motor temperature, and the set temperature of the chiller. The chiller temperature was set to remain constant at 20°C, meaning that the BTMS unit will try to maintain the coolant temperature at this set temperature. The coolant inlet temperature was the actual temperature that comes out of the chiller to cool the components in the circuit. The motor temperature and the drive inverter hot spot temperature show a significant fluctuation, with peak temperature reaching above 90°C, indicating that these components are experiencing high thermal loads during driving.

Figure 29 displays the torque output of the motor over time during the endurance drive run. The torque fluctuates significantly between positive and negative values, indicating acceleration and braking (regenerative braking) phases. The fluctuations imply the vehicle undergoes periodic high-load conditions from the acceleration of moving the truck and deceleration during regenerative braking. The temperature peaks in the drive inverter and motor in Figure 28 appear to correlate with the high torque output seen in Figure 29, suggesting increased heat generation during high power demand.

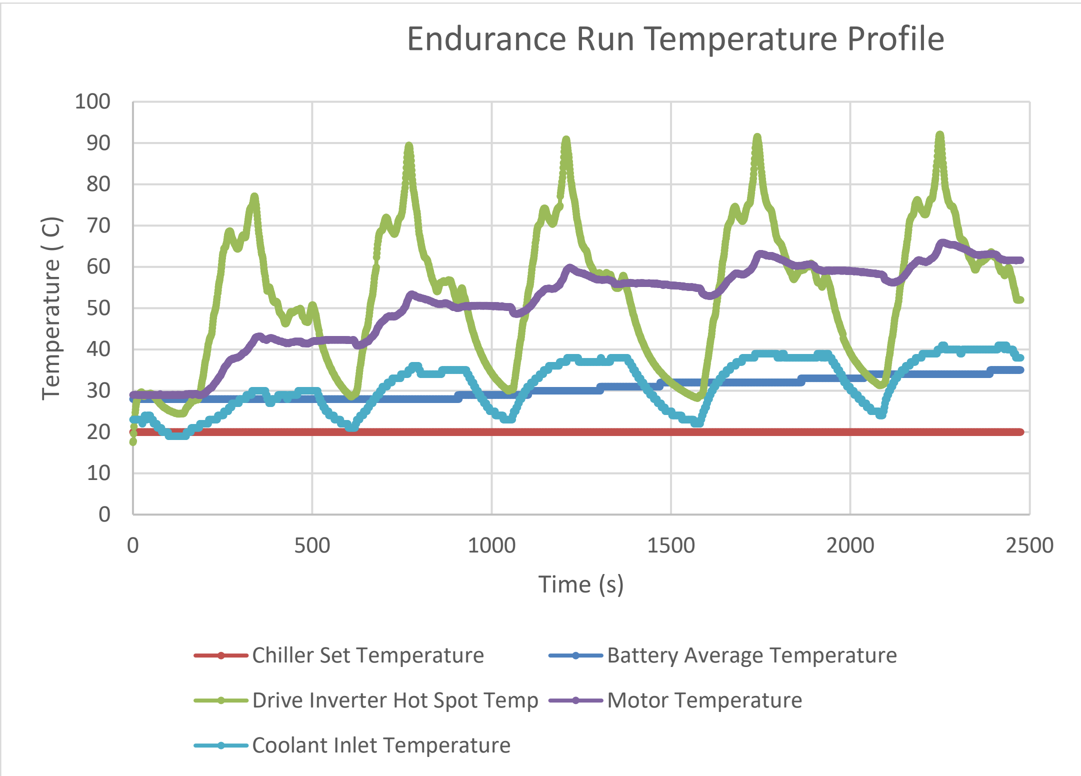

Figure 27: Endurance Run Motor and Inverter Temperature Profile

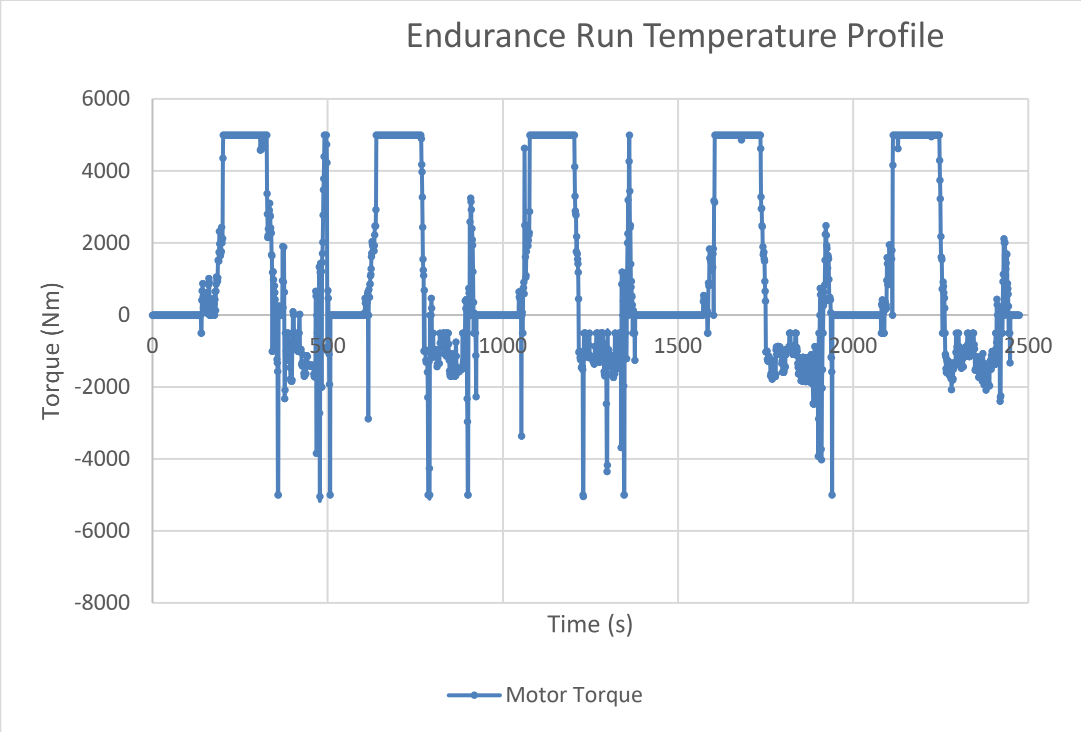

Figure 28: Endurance Run Total Motor Torque Output

4. Discussion

4.1. Orifices Opening Percentage Test

Test 1 focuses on determining the ideal control orifice opening percentage of the auxiliary motor line, drive motor line and battery line. The test results provide valuable insights into the effectiveness of varying orifice opening percentages on the thermal performance of the critical powertrain components, particularly the inverter and battery systems. The test began with all orifices fully open at 100%, which resulted in the highest inverter temperature reading of 63°C. This peak temperature was observed particularly during high-load conditions, such as driving up an incline, where the thermal stress on the system was significantly increased due to the spike in power output. The high inverter temperature at full orifice opening suggests that the current cooling strategy was insufficient under sustained heavy load conditions. The battery temperature only reaches 33°C, which suggests that the flow rate into the battery can be restricted and directed towards the drive inverters.

As the test progressed, the orifice openings were incrementally reduced and analysed. At 50% orifice opening for the heat exchanger and auxiliary drive and 70% for the battery, the inverter temperature dropped to 56.3°C, but the battery temperature slightly increased to 34°C. This trade-off suggests that while reducing the flow to the inverter improved heat dissipation in one area, it may have resulted in a slightly lower heat dissipation within the battery system. However, as the orifices were further reduced to 20% for the heat exchanger and auxiliary drive and 25% for the battery, a more noticeable drop in inverter temperature was observed, reaching 47.5°C, while the battery temperature remained at 34°C.

Despite the improvement in thermal performance, the opportunity for further improvements can be implemented to reduce the temperature of the inverter to below its derating limit of 45°C. The final test configuration, with the heat exchanger and auxiliary drive orifices set to 10% and the battery orifice at 20%, resulted in an inverter temperature of 43.2°C and a battery maximum temperature of 36°C. This configuration successfully lowered the inverter temperature below the first derating threshold, which was a crucial objective of the test. However, the battery temperature increased slightly to 36°C, indicating that further reductions in flow might begin to negatively impact battery thermal management.

From a performance standpoint, these results indicate that a balanced orifice control configuration was crucial to achieving optimal cooling for both the inverter and battery system. While fully opening the orifices settings may translate to a more even cooling performance to all components, systematically reducing orifice openings can help optimise coolant distribution, ensuring that the inverter temperature remains within acceptable limits while preventing excessive buildup in the battery. Additionally, the progressive decrease in inverter temperature with reduced orifice opening suggests that the cooling system was more effective when the flow was maximised towards the drive inverters, which results in improved heat transfer efficiency.

4.2. Chiller Temperature Validation Test

The chiller temperature validation test was conducted to verify the accuracy of the coolant temperature readings recorded by the chiller's built-in sensor against an external Fluke temperature probe. The test setup involved installing the temperature probe at the chiller outlet and running the system at a fixed set temperature of 20°C for 5 minutes. The purpose of this test was to determine whether there were any discrepancies between the temperature readings of the chiller sensor and the Fluke probe, which could help identify and indicate potential calibration errors, sensor placement effects, or thermal lag in the system.

The recorded results show that the HMI consistently logged a temperature of 20°C, reflecting the chiller's setpoint. However, the Fluke probe recorded an average temperature of 20.19°C, displaying a slight discrepancy. The graphical representation in Figure 27 illustrates this difference, where the chiller's temperature remains stable while the Fluke probe data fluctuates slightly around the 20°C mark, with the occasional peaks exceeding 20.6°C. These fluctuations suggest that the temperature probe may be more sensitive to small variations in coolant temperature, potentially due to localised flow variations or slight temperature stratification at the chiller outlet port.

Despite the minor discrepancy, the average difference of 0.19°C was within an acceptable range for industrial cooling applications, indicating that the chiller sensor and the external Fluke probe readings are consistent and in agreement. The fluctuations in the Fluke probe readings could be attributed to the sensor's sensitive response time, which can be caused by the probe positioning or varying coolant flow. However, the overall consistency between the two measurements confirms that the chiller was effectively maintaining the set temperature, and its built-in sensor provides a reliable temperature reading for operational monitoring.

To further improve the measurement accuracy, future tests could investigate different probe placements, improve insulation around the probe, or include an averaging technique to filter out the minor temperature fluctuation readings. Additionally, validating sensor calibration over a broader temperature range could help identify whether this small discrepancy persists under different operating conditions. Nonetheless, the results confirm the accuracy of the chiller's internal temperature probe reading, reinforcing confidence in the reliability of the gathered temperature data.

4.3. Pressure and Flow Test

The coolant flow test provides critical insights into the flow distribution and pressure characteristics throughout the cooling system. These parameters are essential in understanding the efficiency if heat dissipation rate across various components, including the drive motor, inverters, battery, and heat exchangers. The total inlet manifold pressure at PI 01 was measured at 0.9 Bar, which represents the main system pressure at the coolant entry point.

The flow rate readings at various points in the circuit indicate how coolant was distributed across different components. The total flow rate of 46 LPM suggests that a significant portion of coolant was directed toward the drive motors and inverters - since they generate the highest thermal loads during driving. The battery cooling loop receives a moderate share of the coolant flow, while the heat exchanger and auxiliary line have lower flow rates at 4 LPM and 3LPM, respectively. The lower flow rate on the auxiliary line was the result of the lower control orifice opening since they are expected to generate less heat, which will require less cooling than the primary powertrain components. However, depending on the operational conditions, such as hoisting, it may be necessary to ensure that the auxiliary line cooling remains sufficient under extended or high-load use. Similarly, the lower flow rate in the heat exchanger was because the brakes and transmission oil operating oil temperature can reach up to 130C. Moreover, the oil temperature was not expected to reach its high temperature due to the presence of regenerative braking and the removal of the torque converter from the drive line system, which would generate the most heat on the existing diesel truck.

The pressure readings along the circuit provide insight into coolant circulation and pressure drop across the drive motor and inverter lines. The pressure readings suggest a consistent pressure drop across the inverters (~0.08-0.11 Bar), indicating stable coolant flow and effective heat transfer within these components. The pressure drop was expected due to the internal structure of the cooling channel and the significant thermal loads generated by the inverters and drive motors during operation.

The results of this test demonstrate that the cooling system can effectively deliver the required coolant to manage heat dissipation across major components like the drive motors and inverters while maintaining consistent flow to the battery and auxiliary circuits.

4.4. Drive Inverter and Motor Thermal Performance Test

The endurance run test provides valuable insights into the thermal behaviour and cooling performance of the system under real driving conditions. Figure 28 presents the temperature profile of the major components, such as the drive inverter "hot spot" temperature, motor temperature, battery average temperature, and coolant inlet temperature. The inverter "hot spot" temperature was a model developed by the OEM to protect the inverter from overheating during high-power operation. Note that the hot spot temperature was not a direct physical temperature measurement but rather a modelled value used by the OEM inverter as a built-in protection system. This model estimates the thermal stress within the inverter by considering parameters such as motor current, coolant temperature, and available peak current. The inverter's control system then regulates its maximum allowable current output based on this estimated hot spot temperature. The target limit for this model was typically 125°C, and once this limit was approached, the inverter will begin derating power to prevent overheating.

Figures 28 and 29 display the endurance run plot demonstrating the relationship between the inverter hot spot temperature, motor temperature, and torque output. The chiller set temperature was fixed at 20°C, ensuring the BTMS chiller unit attempts to maintain coolant inlet temperature near this level. However, despite the stable coolant inlet temperature, the motor and inverter hot spot temperature exhibit significant fluctuations, with peaks exceeding 90°C during high power demand. This behaviour was consistent with the inverter's internal thermal model, where high current loads result in increased modelled hot spot temperatures, potentially leading to power derating to protect the inverter hardware.

The motor torque profile in Figure 29 showed repeated fluctuations between positive and negative values, reflecting acceleration and regenerative braking cycles. These high torque events correspond with temperature spikes in the inverter and motor, indicating that higher electrical and mechanical loads contribute to increased thermal stress. As the hot spot model reacts to these conditions, it influences the inverter's power output by dynamically limiting current when necessary to avoid exceeding the safe thermal limits.

Overall, this test reinforces the strong correlation between motor load, inverter hot spot temperature, and cooling system effectiveness. While the hot spot temperature model provides valuable protection, further improvements in cooling and power management could enhance the inverter's long-term reliability and efficiency in demanding endurance conditions.

5. Conclusions

To conclude, the current cooling system configuration demonstrated effective thermal management capabilities, particularly in maintaining the temperature of the components in the system below ambient temperature. However, while the chiller can manage the thermal load initially, its effectiveness diminishes over time due to the high heat generation rate from critical power components such as the drive motor and inverter. As the system operates under sustained high loads, such as accelerating and decelerating during driving, the heat generation rate eventually exceeds the cooling capacity of the chiller, causing a gradual increase in coolant temperature. Once the coolant temperature rises beyond a certain threshold, the cooling efficiency declines, leading to an elevated coolant temperature coming out of the BTMS chiller unit. This can result in performance limitations, reduced efficiency, and the introduction of thermal stress on the BTMS chiller unit. To ensure long-term operational reliability of the vehicle, its cooling system must be modified to account for the varying thermal behaviour of the components in the system.

6. Recommendations for further work

An efficient thermal system for a battery electric vehicle was crucial to ensure the truck's critical components operate within the optimal temperature ranges. Based on the research analysis, the following design improvements are recommended to enhance the cooling system's performance, reliability, and adaptability to varying operational conditions.

The current BTMS chiller unit was not sufficient to handle the thermal load of the multiple components in the system. The heat generation rate of all the components exceeds the chiller cooling capacity, which results in a gradual increase in coolant temperature coming out of the chiller over time. The significant finding of the research was that a BTMS chiller was specifically built to manage the temperature of battery packs and not built for other power electronics such as the drive motor and inverters. This was because the heat generation rate of batteries was typically lower, and the rise in temperature was not as drastic as that of other components. The refrigeration system in the chiller cannot handle the sudden temperature spike generated by the power electronics, such as the inverter and motor pair. Therefore, relying on the BTMS chiller unit to cool these components will lead to subsequent damage to the BTMS unit, causing inadequate heat dissipation, which could compromise the system's performance. Therefore, a separate cooling approach tailored to the thermal demands of these high heat-generating components was necessary. A suggestion was to use a radiator air-blast unit to manage the temperature of the drive motors and inverters thermally, the auxiliary motors and inverters, and the brakes and transmission heat exchangers. The major trade-off of a radiator air-blast unit was its inability to reduce the coolant temperature below the ambient temperature, limiting some of the components that can be included in the air-blast circuit. Therefore, it was crucial to assess the impact of high ambient temperatures on the cooling performance of this system to ensure its effectiveness under extreme environmental conditions.

Currently, a common manifold was used in the cooling system to distribute the coolant from multiple chillers to the components in the system. The initial reasoning behind the design was to introduce chiller redundancy to the system by connecting multiple chillers to a common manifold. In the event one chiller was malfunctioning, the other chiller was still capable of delivering the required cooling to the components. However, such a design can introduce preferential flow into the chiller pumps. Due to the presence of pressure differences, some chillers may receive more coolant than others, leading to inefficiencies in the cooling system. Therefore, the design must be changed to mitigate the preferential flow. The BTMS chiller must be directly connected to one or more batteries, ensuring even and controlled coolant distribution. This direct connection will optimise the thermal performance of the system and reduce inconsistencies in heat dissipation.

By removing the common manifold approach, a new contingency system must be implemented to maintain the truck's operation in the event of system failure. A robust cooling system must include effective contingency measures to prevent catastrophic failures or inefficiencies under unexpected conditions. This could involve redundancy in the cooling components, fail-safe mechanisms to detect temperature rise anomalies, and alternative cooling pathways to maintain the vehicle's performance in case the radiator or chiller malfunctions. These measures will enhance system reliability and ensure continued operation under varying loads and environmental conditions of a mining site in Australia.

Once the cooling system was separated into the BTMS chiller circuit and Air-blast circuit, another improvement to consider was incorporating an off-board cooling system. This approach relies on an off-board cooling system for charging rather than having all the available BTMS unit cooling capacity on the truck. The BTMS can then be specified for the heat generation during operation, which was expected to be less than charging. According to the heat generation of the battery pack, the battery will exhibit the highest heat generation during charging at 500A for each battery pack. Conversely, each battery will draw significantly lower power during driving. This design approach will significantly reduce the number of chillers mounted on the truck, leading to a more space and energy-efficient vehicle during operation. During charging, additional outboard BTMS units will be connected to the onboard cooling system to provide the required cooling capacity. In order to implement this design, it was crucial to gather more driving and charging data at different operating conditions. The data must be used to validate the optimised design through calculations and numerical simulations. Moreover, the outboard chiller must be incorporated with the charger to streamline the charging process. The research team must be mindful that such a design will complicate the onboard cooling circuit design, like creating preferential flow when the additional pumps are connected and potential failures in the fittings.

In conclusion, implementing these future design improvements will ensure a more efficient cooling system that was capable of handling the harsh and diverse thermal loads in a mine site and resilient against potential failures, which ultimately will improve the vehicle's performance and longevity.

B.Reff. (2010). Noise and Vibration Refinement of Chassis Suspension. Merkenich-Cologne: Vehicle Noise and Vibration Refinement.

Sudmeyer, R. (2016, 11). Climate in the Pilbara. Retrieved from Department of Primary Industries and Regional Development: https://library.dpird.wa.gov.au/bulletins/220/#:~:text=It%20is%20classified%20as%20hot,50.5%20degrees%20Celsius%20(%C2%B0C)

Appendix 1

The As-Built Piping and Instrumentation Diagram.

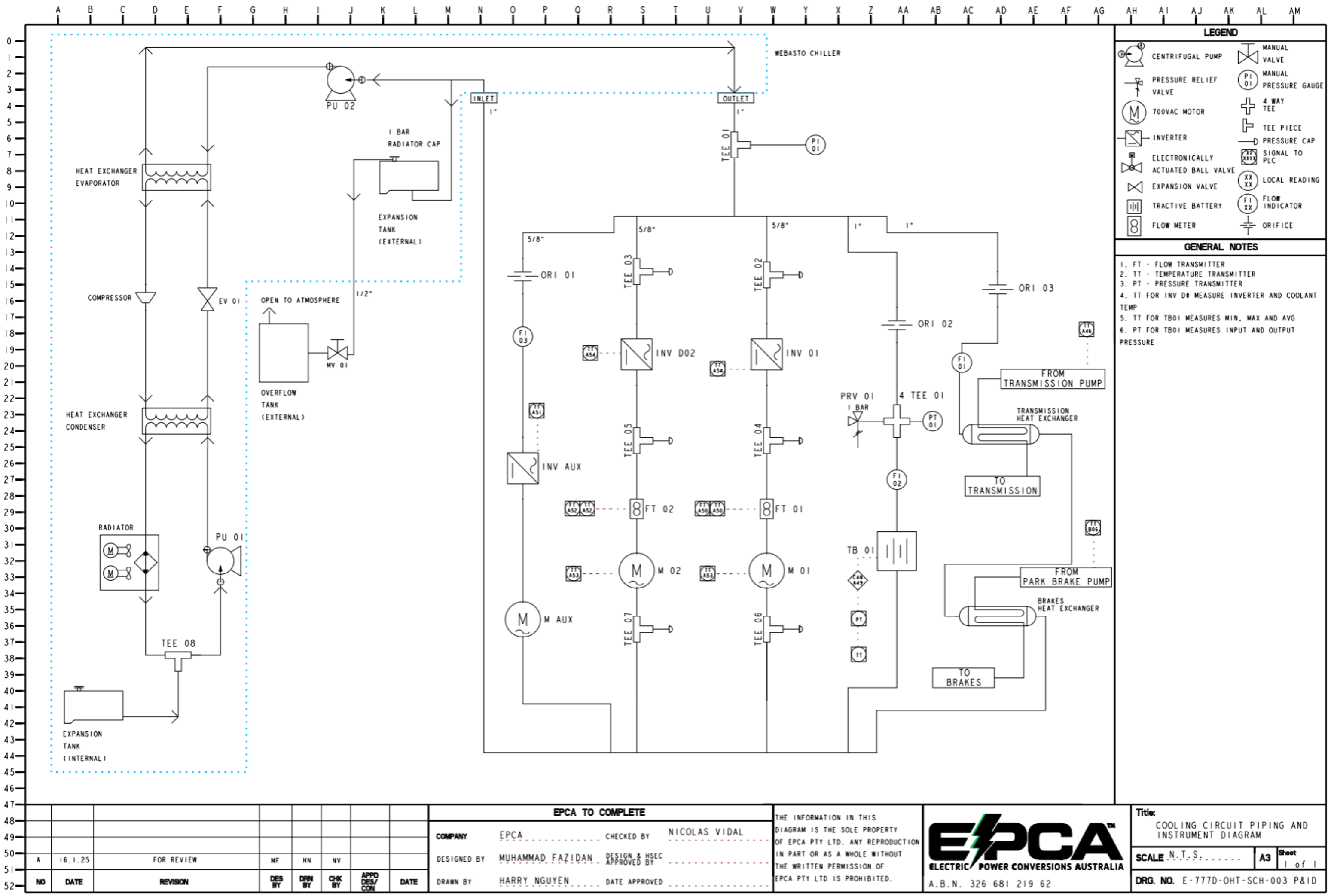

Appendix 2

The digital twin interface properties and parameters are specified in the table below:

- Note that these parameters can be changed at the top-level model and analysed without recompiling the model.

Table 8: EPCA Truck Parameters

Parameters / Variables	Initial Value	Current Value	Notes
Simulator Model	EV_Truck	EV_Truck	
batteryCellInitialSoC	0.95	0.8…0.9	60% or 80% DoD
batteryCellParallel	84	672	84*8 = 8 packs
batteryCellSeries	176	192	
chassisMassKg	55400	55400	
chassisPayloadKg	90000	0…90000	0 kg or 90000 kg
coolerTempTargetK	308.15	308.15	Kelvin (=35°C)
transmissionRatio	47.47	Variable	Dependent on gear
wheelInertia	17600	17600	
wheelMassKg	9600	9600	
wheelRadius	1.35	1.35	
InstanceName	EV_Truck1	EV_Truck1	
UseStartValueInitialisation	false	false	

Battery Pack

- Defined as a single cell (OCV, SOC, and Impedance defined), arranged in a 2D array to model the entire pack.
- 192s672p (8 in parallel) = 129,024 cells total.
- Open Cell Voltage with relation to State of Charge was defined by “CC100E OCV_SOC.csv”.
- 80% Depth-of-Discharge -> 90% max to 10% min.
- 60% Depth-of-Discharge -> 80% max to 20% min.

Machine (Motor/Inverter)

- Defined as a current source on the electrical side, and a torque source on the mechanical side.
- The relation between them was defined with an efficiency map for the controller and another for the motor.

Limits block:

- Max current: 566A per machine (1,698A total for 3 machines)
- Max torque: 2620Nm per machine (7,860Nm total for 3 machines)
- Max power: 425kW per machine (1,275kW total for 3 machines)

Transmission and Wheel

- Transmission was defined as a ratio between the shaft of the motor and the shaft of the wheel assuming no losses.
  - 1st gear -> resultant drive ratio was 85.76.
  - 2nd gear -> resultant drive ratio was 61.26.
  - 3rd gear -> resultant drive ratio was 46.65.
- Wheel was defined by a radius and a rotational inertia (mass was included in the main chassis). The interface between the wheel and the road surface was assumed to be non-slip.

Chassis Mechanics

The chassis mechanics are defined as a combination of the following:

- A force produced by the wheel pushing against the surface.
- A total mass from the sum of the chassis, wheels, and payload.
- An estimate of air friction based on a total frontal area and a coefficient of drag.
- An estimate of rolling friction.
  - Assumption of 200 Ns/m taken from https://www.sciencedirect.com/topics/e (B.Reff, 2010)ngineering/rolling-resistance.
- An additional force due to the current gradient.

Chiller Control

- The chiller itself was the PrescribedHeatFlow block and models a controllable heat flow in or out of the model.
- Thermal loads on the system are defined as a sum of the:
  - Losses in the inverter (Machine).
  - Losses in the motor (Machine).
  - Losses in the battery pack.
- Temperature target was set at 35°C and a PID loop regulates the heat flow in the system.
- 9 chillers with heating function removed.

Gradient Profile (Cycle)

- Defined as a table of values of the gradient (degrees) vs time.
- The angle was converted into a force applied to the chassis (dynamics are only considered in one dimension).
- The average gradient based on the supplied cycle data was calculated to be ±7.69% which was equal to ±4.4°.

Velocity Profile and Torque Control

- Defined by a table of velocity values vs time using the VelocityCycle block.
- The velocityPID loop changes the torque signal sent to the motor to either accelerate or decelerate the vehicle to meet the velocity target.

Scenarios

The following scenarios assume that the BEV should not operate at a faster velocity when loaded, and unloaded speeds are limited by the gear ratios.

- Top speed of 3rd gear was 66.17 km/h.

Scenario 1

Configuration:

- 80% DoD
- Loaded:
    - Velocity Profile: 8.33 (m/s) = 30.00 (km/h)
    - Gradient Profile: -4.4°
    - Payload Weight: 90,000 kg
    - Transient Time: 1600/8.33 = 192 seconds
- Unloaded:
    - Velocity Profile: 18.38 (m/s) = 66.17 (km/h)
    - Gradient Profile: 4.4°
    - Payload Weight: 0 kg
    - Transient Time: 1600/18.38 = 87 seconds

Scenario 2

Configuration:

- 60% DoD
- Loaded:
    - Velocity Profile: 8.33 (m/s) = 30.00 (km/h)
    - Gradient Profile: -4.4°
    - Payload Weight: 90,000 kg
    - Transient Time: 1600/8.33 = 192 seconds
- Unloaded:
    - Velocity Profile: 18.38 (m/s) = 66.17 (km/h)
    - Gradient Profile: 4.4°
    - Payload Weight: 0 kg
    - Transient Time: 1600/18.38 = 87 seconds

Post-Processing

In the below results, there are four individual graphs. The same outputs are measured during each simulation.

- On the first graph State of Charge (SoC) was displayed. Regen was indicated by an increasing SoC.
- On the second graph the Velocity Profile and Chassis Velocity was displayed. The orange dotted trace represents the target velocity set by the PID controller, while the orange trace represents the physical velocity of the BEV.
- On the third graph Motor Torque was displayed. The shown torque was the combined value of the three motors.
- On the fourth graph the Gradient Cycle was displayed. The gradient cycle replicates starting on a flat surface and rising/falling to a gradient of positive or negative slope respectively within 1 second.

Scenario 1

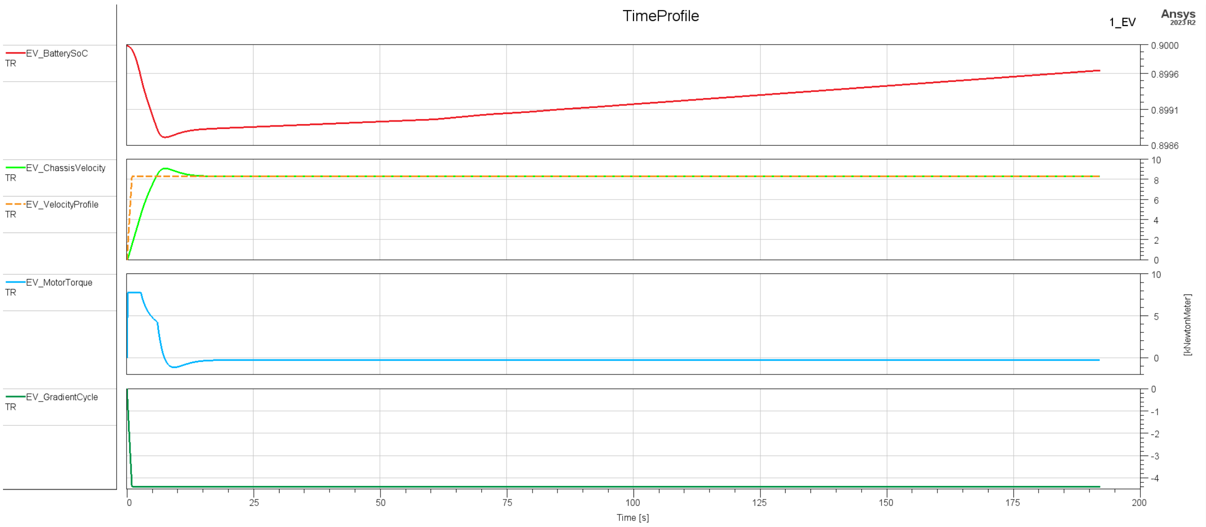

Figure 29: Scenario 1 Loaded

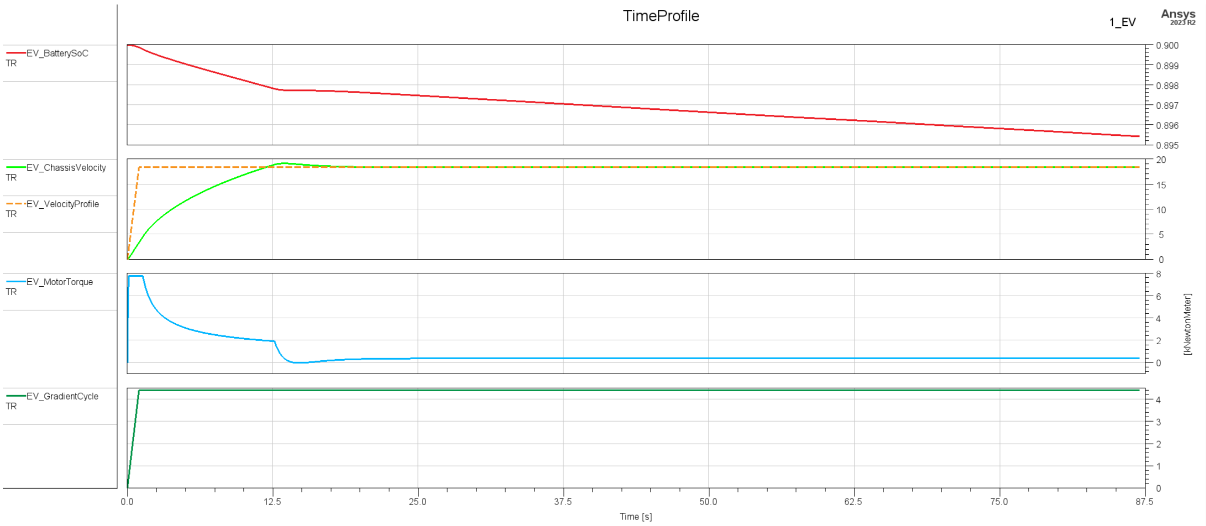

Figure 30: Scenario 1 Unloaded

Scenario 2

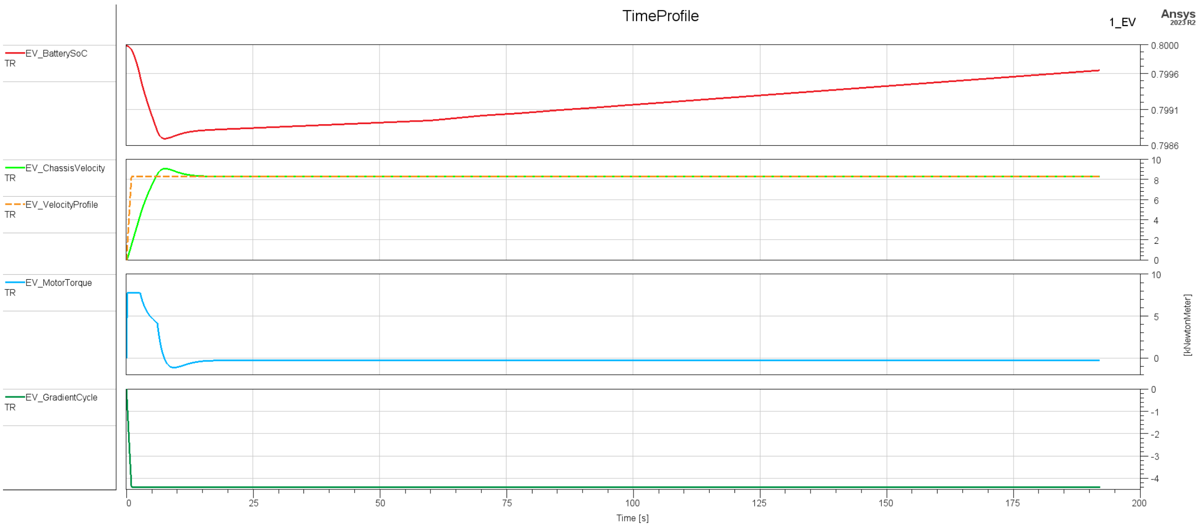

Figure 31: Scenario 2 Loaded

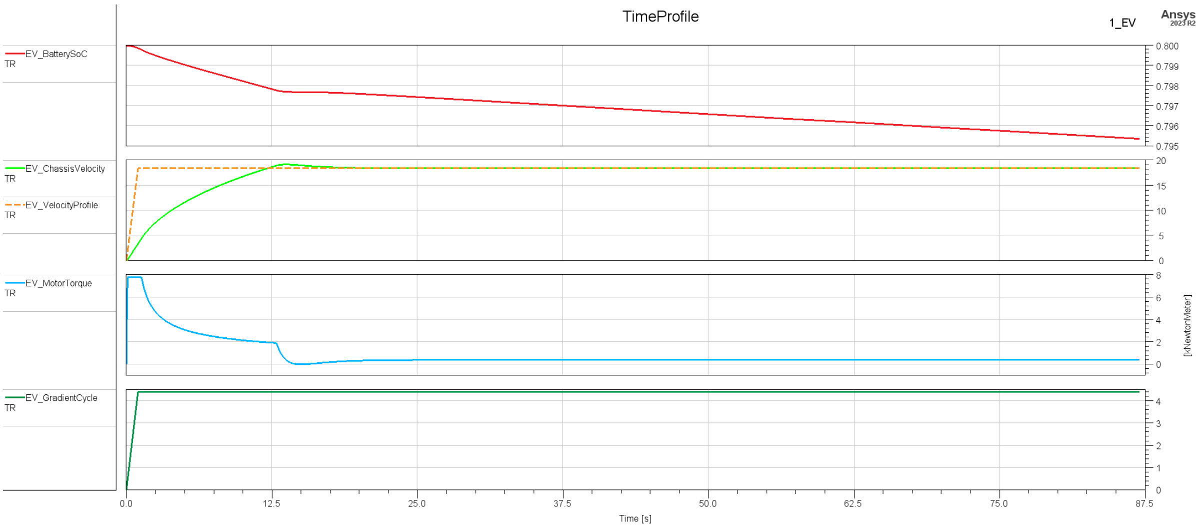

Figure 32: Scenario 2 Unloaded

The below table was calculated with 1 'run' as travelling from the furthest stockpile to the crusher and back.

Table 9: Model Results

Parameter	Scenario 1	Scenario 2
Starting SoC	0.9	0.8
Final SoC	0.89515	0.7948
Delta SoC	0.00485	0.0052
Energy consumed per run (kWh)	11.26	12.08
Time per run (seconds)	279	279
Runs per charge	164	115
Runtime per charge (hours)	12	9